Studying bright variable stars with the Multi-site All-Sky CAmeRA (MASCARA)

Burggraaff, O.; Talens, G.J.J.; Spronck, J.; Lesage, A.-L.; Stuik, R.; Otten, G.P.P.L.; ... ; Snellen, I.A.G.

Astronomy & Astrophysics manuscript no. Burggraaff_arxiv
June 7, 2018

Studying bright variable stars with the Multi-site All-Sky CAmeRA (MASCARA)⋆

O. Burggraaff[1] ⋆⋆, G.J.J. Talens[1], J. Spronck[1], A.-L. Lesage[1], R. Stuik[1], G.P.P.L. Otten[1], V. Van Eylen[1], D. Pollacco[2], and I.A.G. Snellen[1]

[1] Leiden Observatory, Leiden University, PO Box 9513, 2300 RA Leiden, The Netherlands
[2] Department of Physics, University of Warwick, Coventry CV4 7AL, UK

Received day month year / Accepted day month year

ABSTRACT

Context. The Multi-site All-Sky CAmeRA (MASCARA) aims to find the brightest transiting planet systems by monitoring the full sky at magnitudes $4 < V < 8.4$, taking data every 6.4 seconds. The northern station has been operational on La Palma since February 2015. These data can also be used for other scientific purposes, such as the study of variable stars.

Aims. In this paper we aim to assess the value of MASCARA data for studying variable stars by determining to what extent known variable stars can be recovered and characterised, and how well new, unknown variables can be discovered.

Methods. We used the first 14 months of MASCARA data, consisting of the light curves of 53 401 stars with up to one million flux points per object. All stars were cross-matched with the VSX catalogue to identify known variables. The MASCARA light curves were searched for periodic flux variability using generalised Lomb-Scargle periodograms. If significant variability of a known variable was detected, the found period and amplitude were compared with those listed in the VSX database. If no previous record of variability was found, the data were phase folded to attempt a classification.

Results. Of the 1919 known variable stars in the MASCARA sample with periods $0.1 < P < 10$ days, amplitudes > 2%, and that have more than 80 hours of data, 93.5% are recovered. In addition, the periods of 210 stars without a previous VSX record were determined, and 282 candidate variable stars were newly identified. We also investigated whether second order variability effects could be identified. The O'Connell effect is seen in seven eclipsing binaries, of which two have no previous record of this effect.

Conclusions. MASCARA data are very well suited to study known variable stars. They also serve as a powerful means to find new variables among the brightest stars in the sky. Follow-up is required to ensure that the observed variability does not originate from faint background objects.

Key words. stars: variables: general – binaries: eclipsing

1. Introduction

Variable stars–stars that change in magnitude over time–have been a field of study since antiquity (Jetsu et al. 2013). Currently, over 500 000 examples are listed in the International Variable Star Index[1] (VSX). Variable stars are often discovered as a secondary science goal of large stellar survey projects, such as OGLE (Udalski et al. 2015; Soszyński et al. 2008) and the NASA Kepler Mission (Prša et al. 2011), which each have identified thousands of variable stars albeit at relatively faint magnitudes. Astrometric surveys such as Hipparcos (ESA 1997) and currently Gaia (Gaia Collaboration et al. 2016) perform all-sky surveys that include the brightest stars, but only with a relatively low number of measurements per object. A number of other surveys have identified bright variable stars, such as ASAS (Pojmański 2002), KELT (Pepper et al. 2007) and MOST (Pribulla et al. 2008). TESS will provide excellent photometry on stars as bright as $V = 4.5$ mag but will be limited by its mission duration to relatively short period ($P_{\max} \approx 40$ days) variable stars only (Ricker et al. 2015). Additionally, the study of variable stars is one of the richest fields in terms of amateur contributions. Organisations such as the American Association of Variable Star Observers (AAVSO) provide light curves of thousands of stars over periods of decades, based in part on volunteer work. However, coverage is mostly sparse and heterogeneous.

Variable stars have great value across many fields of astrophysics. Pulsating variable stars such as cepheids, have been used to accurately determine distances of deep-sky objects (Hubble 1929). Currently these stars, and other types of variables in the 'instability strip' on the Hertzsprung-Russell diagram, are often used as testing grounds for models of stellar structure and evolution (Groenewegen & Jurkovic 2017; Anderson et al. 2016; Smolec 2016). Eclipsing binary systems provide measurements of the masses and radii of their components to the level of accuracy needed to constrain models of stellar structure. Since any type of star can be part of a binary system, this method allows for measurements of these parameters across the Hertzsprung-Russell diagram, rather than only specific sections of it (Torres et al. 2010). Space missions such as BRITE are now capable of observing many such stars with high precision, short cadence and over long time scales (Weiss et al. 2014).

In this paper we wish to assess how valuable Multi-site All-Sky CAmeRA (MASCARA) data are to study variability in bright stars. As far as we know, MASCARA is currently the only survey that monitors the near-entire sky at $V < 8$ magni-

⋆ Tables A.1 and B.1 are also available in electronic form at the CDS via anonymous ftp to cdsarc.u-strasbg.fr (130.79.128.5) or via `http://cdsweb.u-strasbg.fr/cgi-bin/qcat?J/A+A/`.

⋆⋆ e-mail: `burggraaff@strw.leidenuniv.nl`

[1] `https://www.aavso.org/vsx/`

tudes. In Sect. 2 we discuss MASCARA and its data. In Sect. 3 the analysis is presented, in which we determine the recovery rate of known variable stars in the first 14 months of data. Furthermore, the MASCARA data is searched for new yet-unknown variables. In Sect. 4 the results are presented, which are discussed in Sect. 5.

2. MASCARA data

The main goal of the Multi-Site All-Sky CAmeRA (MASCARA) is to detect exoplanets around bright stars using the transit method. The northern-hemisphere MASCARA station, located on La Palma (Canary Islands, Spain), has been fully operational since February 2015. The southern station, located at La Silla (Chile), saw its first light in June 2017. Thus far, two exoplanets have been discovered using MASCARA data (Talens et al. 2017a,b).

Each MASCARA station contains five cameras, one pointed in each cardinal direction and one at zenith, covering the local sky down to airmass two to three. The cameras are modified Atik 11000M interline CCDs, without a filter, giving them a spectral range of approximately 300 to 1000 nanometres. Each camera is equipped with a Canon 24 mm $f/1.4$ USM L II lens with a 17 mm aperture, providing a $53° \times 74°$ field of view each, at a scale of approximately 1 arcminute per pixel. For a detailed description we refer the reader to Talens et al. (2017c).

The cameras take 6.4 second back-to-back exposures through the night at fixed local sidereal times. Aperture photometry is applied to these images to extract the fluxes of all the stars with $V < 8.4$ mag. This is done automatically for a list of stars known to be visible with MASCARA, based on the All-Sky Compiled Catalogue (ASCC; Kharchenko 2001). These measurements are binned in groups of 50, producing a light curve with a binned data point every 320 seconds. A detailed description of the MASCARA data reduction pipeline and analysis is presented in Talens et al. (in prep.).

Our analysis is based on the first year of data of the northern station, taken between February 2015 and March 2016 (heliocentric Julian dates (HJD) 2 457 056 – 2 457 480). The data set consists of up to 25 000 binned data points (HJD, magnitude, magnitude error) per star, with a median number of binned data points of 12 757 ($\approx$ 1100 hours). The number of flux points for a given star depends mainly on its sky coordinates, in particular its declination. The stars range in right ascension from 0^h to 24^h, in declination from $-38.6°$ to $+90°$, and in V-magnitude from 2.0 to 8.4. We note that the brightest stars, with $V < 4$ mag, are likely to be saturated at certain parts of the CCDs, effectively reducing the number of usable data.

3. Analysis

Our MASCARA data analysis consists broadly of four steps, applied to each star individually. Firstly, an ansatz period of variability was searched for through the generalised Lomb-Scargle periodogram (GLS; Zechmeister & Kürster 2009) of the MASCARA light curves. Secondly, systematic effects caused by the instrument and the Moon were removed. Thirdly, a direct χ^2 minimalisation was performed to obtain the final estimate for the period of variability. Finally, the candidate variable star was checked for being a false positive caused by variability of a known background star. All analysis was performed using designated python scripts.

3.1. Step 1: Finding the Ansatz period

A first estimate for the strongest periodic signal in a light curve was determined through the generalised Lomb-Scargle periodogram (GLS; Zechmeister & Kürster 2009), a variation on the standard Lomb-Scargle periodogram (Scargle 1982) which allows weighting of data points and fitting of the mean value. This periodogram is equivalent to a χ^2 fit of sine waves to the data. We tested up to 68 000 periods ranging from 640 seconds to 100 days. The upper limit was set to ensure the presence of multiple cycles in the data. GLS power can range between 0 and 1, equivalent to no fit and a perfect sinusoidal fit respectively. The strongest signal in the GLS was used as a first estimate for the true period of variability. Care was taken to ignore signals within 5% of 1 sidereal day or an alias thereof (1/2, 1/3, ... days) and within 5% of 29.5 days, as these are caused by systematic effects as described in step 2.

As an example, the GLS of ASCC 425414 (RR Lyrae) is shown in Fig. 1. The forest of strong signals are all aliases ($f_{\rm alias} = f_0 + k$ with $f_0 = 1/P_0$ and k an integer) and harmonics ($P_{\rm harm} = kP_0$ or $P_{\rm harm} = P_0/k$ with k an integer) of the true period of $P_0 = 0.567$ days, which itself has the strongest power in the GLS diagram of $p_{\rm max} \approx 0.7$.

3.2. Step 2: Removal of systematics

Two important systematic effects are present in the MASCARA light curves. The first has a period of one sidereal day and is caused by the varying PSF of the cameras across their field of view. The second has a period of 29.5 days and is caused by changing background levels due to the Moon. The amplitude and significance of these effects differ between stars and are related to their sky position, magnitude and the amplitude of their variability.

Systematic flux variations with a period of 1 sidereal day are caused by the considerably variable point spread function of a MASCARA camera across its field of view (see Talens et al. 2017c). Since the cameras stare at a fixed position, a star typically travels across the CCD in a few hours, significantly changing the fraction of light that falls within the aperture used to obtain the photometric measurements. Since all flux measurements are obtained relatively to a set of surrounding stars, to first order this effect cancels out. However, since the PSF changes so strongly, faint wings from neighbouring stars enter and leave the aperture according to the position of the star on the CCD – an effect that is unique to each individual object. It will be the strongest for faint stars with very close and bright neighbours and can have amplitudes up to 0.5 in magnitude. Fortunately, the path of a star on the CCD is nearly identical for every sidereal day, and therefore this systematic effect can be measured and removed. An example of such an LST (local sidereal time) trend for the star ASCC 1006099 (EG Cet) is given in Fig. 2.

The 29.5-day effect is caused by the Moon. As the Moon moves across the sky, it significantly affects the local sky. In a way that is not yet completely understood by the MASCARA team, the sky background level influences the measured fluxes, depending on the magnitude of the star. It typically has an amplitude of 0.01 magnitude. Additionally ghost images will appear. These effects are difficult to predict and thus are not removed in the original data pipeline. The resulting effect also has a period of 29.5 days and can have significant amplitudes of up to 0.6 magnitude.

To remove these systematics, firstly the data were phase folded with the ansatz period determined from the GLS (Step

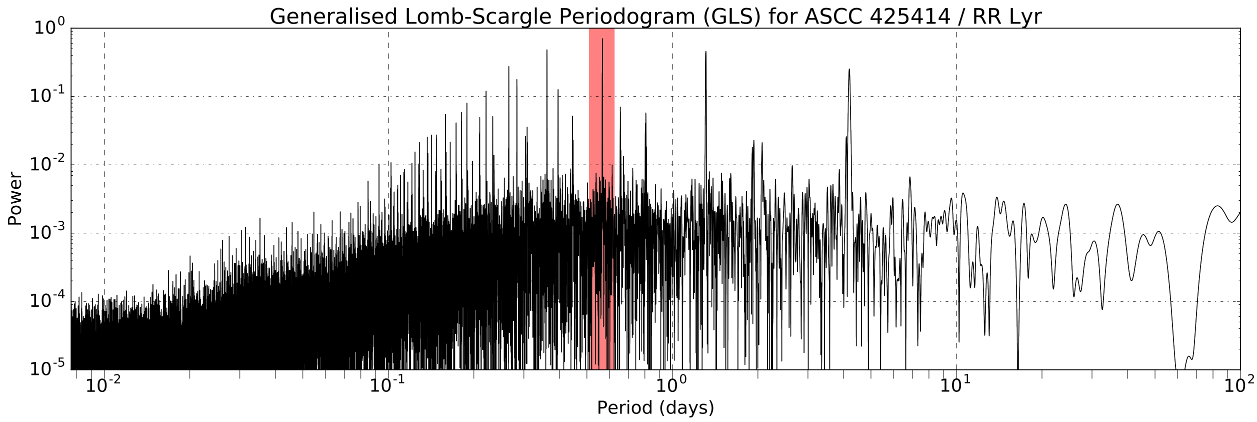

Fig. 1. Generalised Lomb-Scargle periodogram of ASCC 425414 (RR Lyrae). The strongest signal is at a period of $P = 0.567$ days, highlighted with a red background. We note that in this particular case, the instrumental effects discussed in Sect. 3.2 are not strongly present in the GLS.

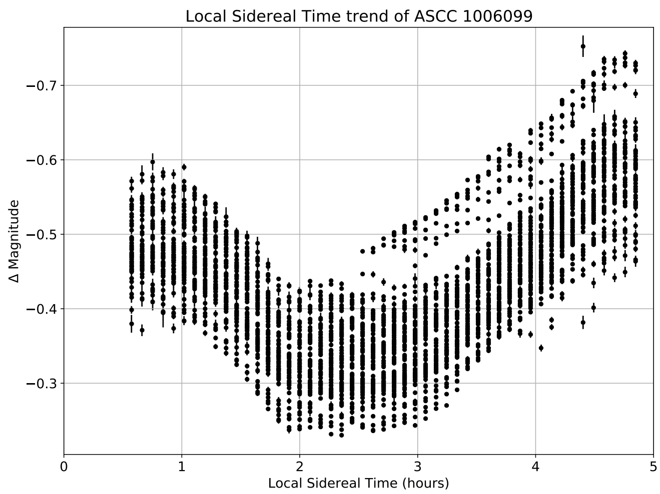

Fig. 2. PSF variations in the zenith camera data for the star ASCC 1006099. The magnitude axis zero-point is arbitrary. We note that the data are taken at fixed sidereal times.

1). The resulting light curve was binned in phase space using 150 bins, and the weighted mean of each bin was removed from the data. The residuals subsequently contained only the LST and lunar trends. First the residuals were phase folded with $P = 29.5$ days, again binned in phase space, and that resulting trend was removed from the original data. The process was then repeated for $P = 1$ sidereal day, removing that trend from the data as well. This was done iteratively until the LST and lunar trends were below 0.001 magnitude in amplitude. The systematics were removed on a per-camera basis while the ansatz period phase-fold was done with data from all cameras combined. The resulting detrended data were used for further analysis.

3.3. Step 3: Final period estimate

In the next step the GLS was calculated again for the detrended data, and its strongest period determined. This was generally very close to the ansatz period from the original GLS, but for a small number of stars the period with the strongest signal after detrending changed – now in line with the literature value. Also, since in general the light curves do not resemble sinusoids, the period determined from the GLS may differ slightly from the real period.

We therefore repeated the phase fold and binning procedure from Step 2 with the detrended data for 1000 periods in the ±0.5% range around the GLS period P_{GLS}, in addition to similar ranges around $2P_{GLS}$ and $4P_{GLS}$ to search possibly better solutions at twice and four times the period. This is important mostly for eclipsing binaries, for which the light curve is more similar to a sine wave (and thus appears stronger in the GLS) when the primary and secondary eclipse are overlaid on each other. In general, only $2P_{GLS}$ and $4P_{GLS}$ were tested because in a sub-sample, no stars were found to have a stronger signal for $0.5P_{GLS}$ or other multiples. Since this χ^2 calculation is a computationally expensive operation, it was chosen to only do 1, 2 and $4P_{GLS}$. The final period was chosen to be that with the lowest χ^2 of the phase-folded binned data points with respect to the binned-averaged light curve. The uncertainty interval on the final period estimate was determined from the χ^2 curve using standard methods.

For a small sub-set of the new variable star candidates and known variable stars with new parameters determined by MASCARA, namely 26 out of 492 stars, manual adjustment of the period was necessary. These were generally long-period variables of which the period needed to be halved and eclipsing binaries with elliptical orbits, which cause a phase difference between primary and secondary eclipse significantly less than 0.5. For these stars, the range for the χ^2 calculation was manually adjusted based on a visual inspection of the light curve.

3.4. Step 4: Removal of false positives

Due to the low resolution of the MASCARA cameras (1 arcminute per pixel), there is a large degree of blending. This involves the PSFs of two stars overlapping, causing variability from one star to appear in the light curve of the other. For example, ASCC 571737, which is located 14.7′ from ASCC 571833 (RT Aur), has in its light curve an oscillation very similar to that of RT Aur. Both light curves are shown in Fig. 3 for comparison. This blending can lead to false positive detections.

To potentially mitigate this, all known variable stars within a 1° radius of a candidate were examined. If any had a period that is similar to the candidate and a magnitude $m < 12$ in the VSX catalogue, the candidate was rejected. The magnitude limit was chosen to prevent extremely faint variables from causing

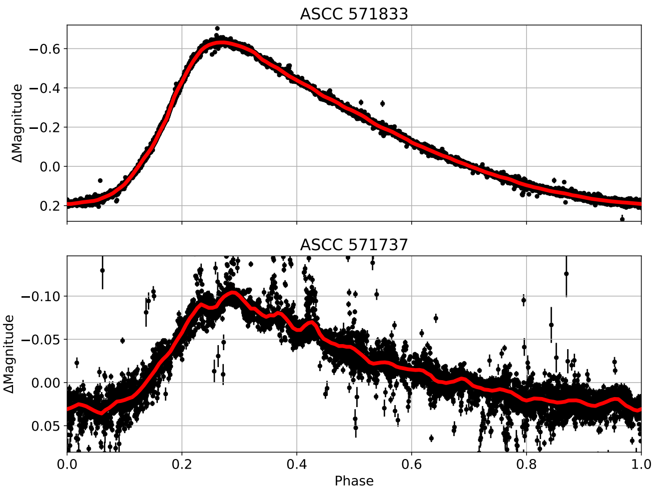

Fig. 3. Comparison between light curves of ASCC 571833 (top; RT Aur) and ASCC 571737 (bottom; HD 45237), both phase folded with the same period $P = 3.72816$ days. The red line is the weighted mean; the magnitude axis zero-points are arbitrary. The period and shape of the light curves are similar but the amplitudes are different: 0.82 vs. 0.13 magnitude. The variability seen in ASCC 571737 is completely caused by that in ASCC 571833.

false negatives. The limit is significantly lower than the lowest magnitude stars MASCARA can detect, but accounts for the heterogeneous nature of the VSX catalogue, which lists magnitudes in various bands.

4. Results

The analysis was first tested on a sample of 2776 known variable stars with recorded periods and amplitudes in the VSX database, after which it was applied to the remainder of the stars in the MASCARA sample. The cross matching between VSX and ASCC was done by finding stars with coordinates within 10″ from each other.

4.1. Recovery of known variable stars

The recovery rate of known variable stars from the VSX database in the MASCARA data is shown in Fig. 4. It depends strongly on the variability amplitude and period. For those stars with periods $0.1 < P < 10$ days and amplitudes > 2% and > 1000 binned data points, 93.5% of the objects are recovered in the first year of MASCARA data. For 40% of the recovered objects, the catalogue and MASCARA periods match within 5%. For amplitudes between 1 and 2%, MASCARA finds 86.2% of the known variables. Of the long period variable stars with $10 < P < 100$ days, MASCARA recovers 68.3% of those known in the VSX catalogue.

The median uncertainty in the final MASCARA period as determined in (Step 3) is three minutes, with a median relative uncertainty of 0.1%. The found uncertainties in the period can be as low as 0.5 seconds for regular high-amplitude variable stars. The phase folded light curve of RR Lyr is given in Fig. 5 as an example of the quality of MASCARA data and the period fitting. The distribution of the residuals is best fit with a Gaussian with $\sigma = 0.028$ magnitude, indicative of the typical uncertainty in the MASCARA fluxes for this star.

4.2. New parameters for known and suspected variables

A further 4236 stars listed in the VSX without a recorded period were analysed. Reliable periods were found for 210 of these, which are listed in Table A.1, with the parameters of the star (identification, coordinates, V-magnitude, number of observations by MASCARA) and of its variability (period, amplitude, epoch, VSX variability type designation). For a subset of these stars, an estimate from the MASCARA light curve of the type of variability eclipsing binary, pulsating, or other) is also included. Light curves and periodograms of seven example stars are shown in Appendix A, and can be found for all stars with new parameters at `https://home.strw.leidenuniv.nl/~burggraaff/MASCARA_variables/`.

One interesting example of a previously suspected variable star recovered with MASCARA is ASCC 408281 (HD 101207). HD 101207 is a known binary system, consisting of a component A with $V_A = 8.11$ mag and a component B with $V_B = 9.32$ mag, with a visual separation of 1.97 arcsec (Fabricius et al. 2002). This separation is much smaller than the MASCARA pixel size (which is approximately 1 arcmin), so the two stars are fully blended in the MASCARA data. The system has an orbital period of approximately 4000 years (Malkov et al. 2012). HD 101207B is identified in the ASCC-VSX cross match with the suspected variable star NSV 5279.

The MASCARA data for HD 101207 show a clear periodicity, with a best period estimate of $P = 1.09014(5)$ days. The phase folded light curve is given in Fig. 6. This light curve clearly shows a single dip with an amplitude of 104 mmag, and the system can be easily identified as an eclipsing binary (EB). This feature cannot be explained by the previously known double nature of the HD 101207 system, since the orbital period of the A and B components is 4000 years.

As noted in Sect. 3.4, blending due to the low resolution of the MASCARA cameras can cause false positive detections. However, only two systems with $V < 10$ mag were found within a 10 arcmin radius from HD 101207: BD+42 2231 and BD+41 2217. The latter has a separation from HD 101207 of 4.5 arcmin and is too faint ($V = 9.20$ mag) to cause significant blending effects at that separation. BD+42 2231 has a separation from HD 101207 of 2.2 arcmin and a V-magnitude of 9.10. The small separation (2 pixels) means some blending between the stars will occur, but due to the faintness of BD+42 2231, it is very unlikely to induce a variability with an amplitude as high as 104 mmag in HD 101207. BD+42 2231 is a known spectroscopic binary, but its orbital period is 951.5 ± 2.1 days (Pourbaix et al. 2004), too long to explain the variability seen in HD 101207.

Thus the most likely explanation for the observed variability is a previously unknown binary nature of one of the components of HD 101207. Since component A is significantly brighter than B ($V_A = 8.11$ mag compared to $V_B = 9.32$ mag), it is likely that HD 101207A is the eclipsing binary component. However, this cannot be said with certainty due to the complete blending of the two components in the MASCARA data. We expect that the MASCARA data contain many of such as yet undiscovered systems.

4.3. New MASCARA candidate variable stars

Finally the 45 749 stars in the MASCARA sample with sufficient data that are not listed in the VSX catalogue were analysed. Periodic variations were detected in the light curves of 438 of these stars. Checks against the VSX catalogue for background variables (Step 4) revealed 156 false positives, leaving 282 as new

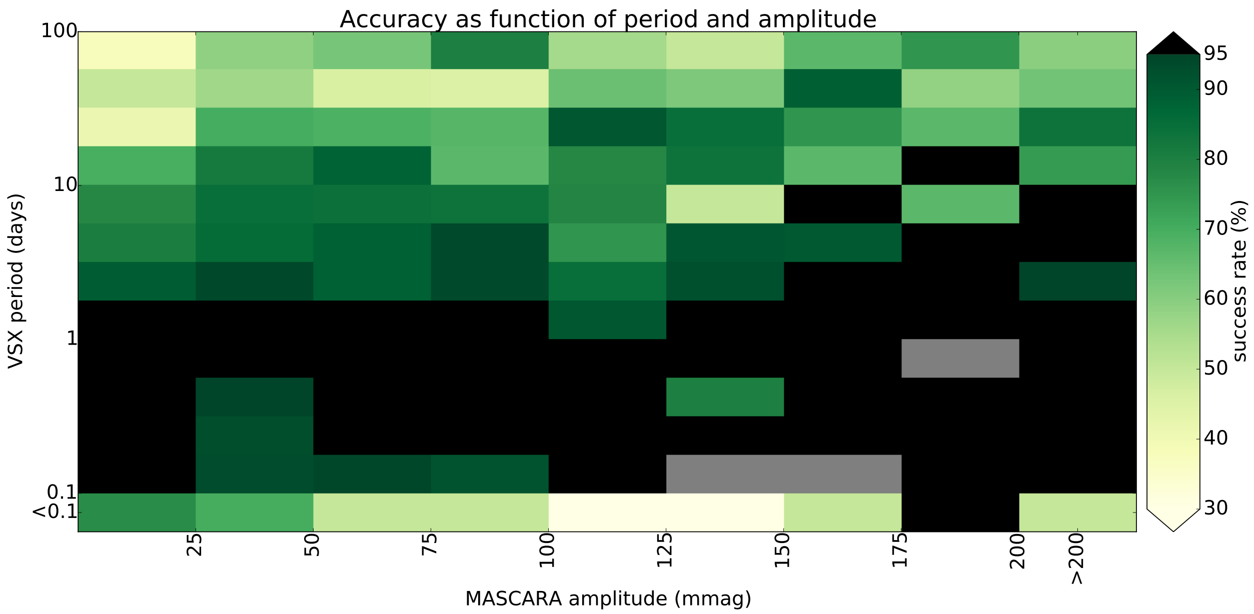

Fig. 4. Recovery rate of known variable stars in the MASCARA data as a function of period and amplitude of the variability. Black rectangles have a success rate > 95%; grey rectangles contain no stars.

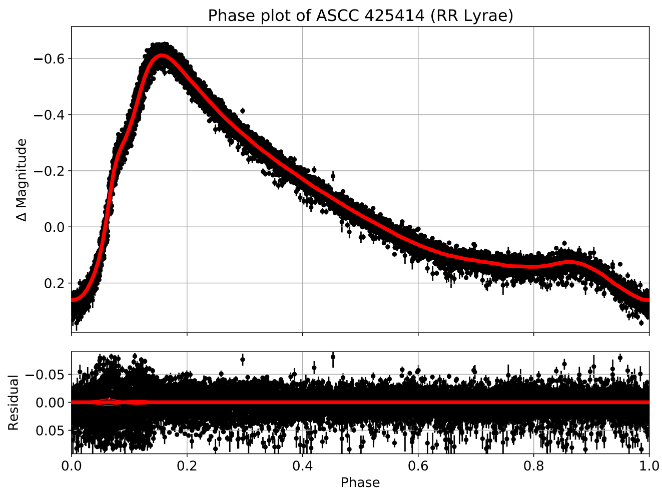

Fig. 5. MASCARA light curve of 13 279 binned data points of RR Lyrae phase folded with a period of 0.566774 days. The red line is the running average over an 0.025 phase interval. For clarity, the data are clipped at 3-σ from the running mean, removing 2.1% of the binned data points.

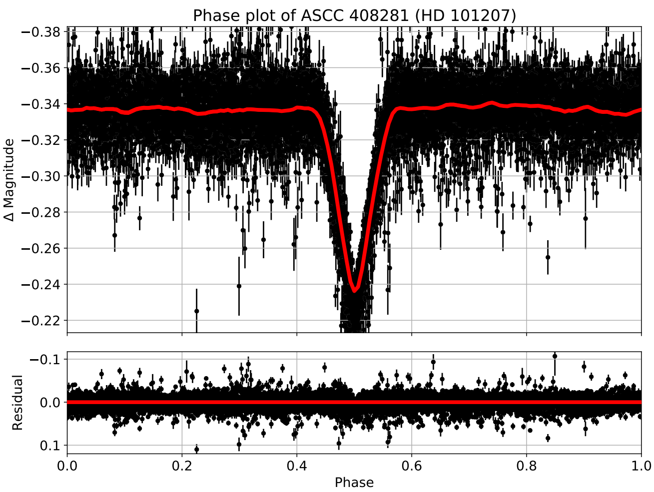

Fig. 6. MASCARA light curve of ASCC 408281 (HD 101207), a previously suspected variable, which was detected with MASCARA, with a period of 1.09014(5) days. The red line is the running average over an 0.025 phase interval. The light curve clearly shows a single eclipse-like feature.

MASCARA candidate variable stars listed in Table B.1. As with the known variable stars discussed in Sect. 4.2, an estimate of the type of variability of these stars (eclipsing binary, pulsating or other) was made based on their MASCARA light curves. 44 were visually identified as possible eclipsing binary systems.

Light curves and periodograms for seven example new candidate variables are included in Appendix B, and can be found for all candidates at `https://home.strw.leidenuniv.nl/~burggraaff/MASCARA_variables/`. The reader should note that these stars still need to be vetted with further observations.

An interesting example of a new candidate variable star is ASCC 201832 (TYC 3926-224-1). This star is not known in the extended literature to have a variable or binary nature. Though it is a relatively bright star (V = 7.42 mag), it was not included in the Hipparcos catalogue (ESA 1997). It has been included, but not flagged as a variable star, in the second Gaia data release (Gaia Collaboration et al. 2018; Holl et al. 2018).

The MASCARA light curve of TYC 3926-224-1, given in Fig. 7, shows a clear variability with a period P = 0.61747(5) days. The light curve is similar to that of β Lyr type variables, with a primary and secondary eclipse, and a continuous change in brightness over the whole period. The depth of the primary eclipse is 160 mmag, while the depth of the secondary eclipse is 81 mmag.

No stars significantly brighter than TYC 3926-224-1 were found within a degree from it. There are only two stars with V < 8 mag within a radius of 40 arcmin, with separations of 8.6 and 9.0 arcmin. Neither of these stars, HD 173700 and HD 173605

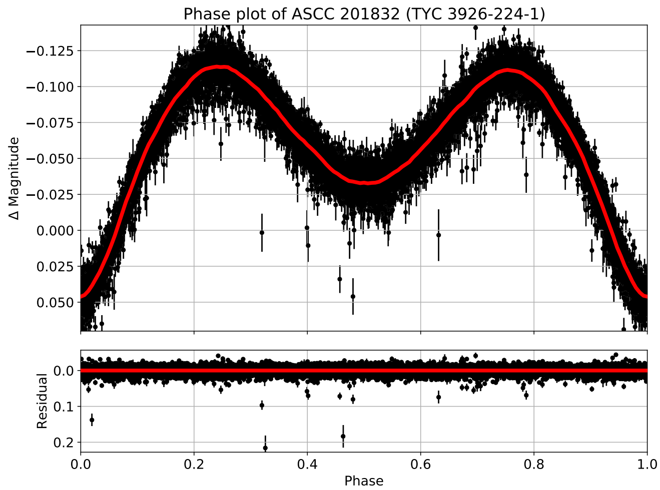

Fig. 7. MASCARA light curve of ASCC 201832 (TYC 3926-224-1), a new variable star candidate with a period of 0.61747(5) days. The red line is the running average over an 0.025 phase interval. The light curve clearly shows a primary and secondary eclipse.

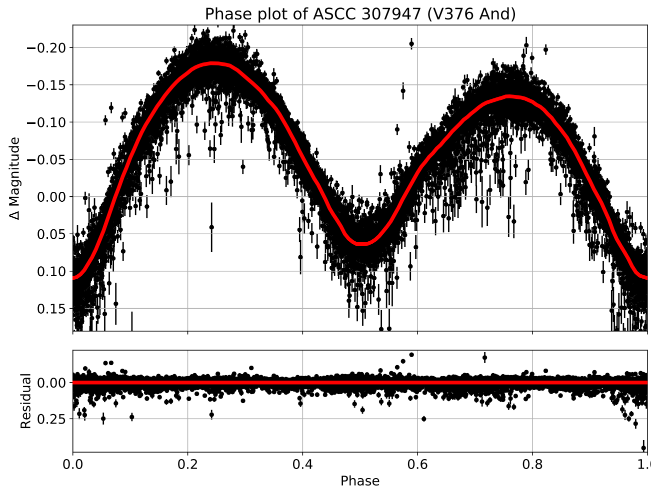

Fig. 8. Light curve of ASCC 307947 (V376 And), a known β Lyr type eclipsing binary with a period of 0.79867(6) days. The O'Connell effect is visible as a difference in magnitude between the two maxima. The red line is the running average over an 0.025 phase interval.

respectively, is known or suspected to be variable. Since both are fainter than TYC 3926-224-1 and the separations are sufficiently large, it is unlikely that the variability seen in TYC 3926-224-1 is due to blending with either of these stars.

There is one suspected variable star within 10 arcmin of TYC 3926-224-1, namely NSV 24573 (HD 173603). This star was flagged as variable in the Hipparcos catalogue but has not been flagged by Gaia (ESA 1997; Gaia Collaboration et al. 2018). Variability in this star was also detected with MASCARA, with a period of 3.63(2) days and an amplitude of 37 mmag. Thus it is unlikely that blending with HD 173603 has caused the variability observed in TYC 3926-224-1.

Since no likely blending candidates were found, it can be concluded that TYC 3926-224-1 itself is likely a new variable star. Given the shape of its light curve, it is likely an eclipsing binary of the β Lyr type. However, we stress that follow-up observations are necessary to confirm its being variable.

4.4. Detailed variability studies

We also investigated to what extent particularly second order effects in the light curves of variable stars can be studied using MASCARA data. For this we focus on the O'Connell effect in eclipsing binaries.

The O'Connell effect is an asymmetry in the brightness of the two maxima in the light curve of an eclipsing binary system, of which the physical cause is not yet well understood (O'Connell 1951; Wilsey & Beaky 2009). It occurs in eclipsing binaries of the β Lyr and W UMa subtypes, with the maximum after the primary eclipse being brighter than that before the primary eclipse.

An example MASCARA light curve of a star showing this effect, the β Lyr variable V376 And, is given in Fig. 8, with the first maximum approximately 0.05 mag brighter than the second. Table 1 contains a non-exhaustive list of known eclipsing binaries in the MASCARA sample exhibiting a significant O'Connell effect. The effect is not detected in any of the newly found variables.

5. Discussion and conclusions

To our knowledge, MASCARA is the first instrument to accurately monitor the near-entire sky, recording the flux of all bright stars ($V < 8.4$ mag) down to airmass two to three every 6.4 seconds. Typical precisions of 1.5% per five minutes are reached at the faint magnitude end. With the analysis presented here we show that MASCARA data are very well suited to study known variable stars and can serve as a powerful means to find new variables among the brightest stars in the sky.

Using a generalised Lomb-Scargle analysis we show that 93.5% of all known variables with periods between 0.1 and 10 days and amplitudes > 2% are recovered using the first year of MASCARA data. However, great care has to be taken to remove systematic effects in the data, in particular with periods of one sidereal day and aliases thereof. Hence, identifying and studying stars that exhibit variability with a period at or near 1.0 day will be very challenging with MASCARA data alone.

The recovery fraction of known variable stars drops significantly below periods of 0.1 day (158/231 = 68%). We note that short period variables often show multi-periodicity and irregular light curves, which are therefore more challenging to detect using a Lomb-Scargle analysis. For the MASCARA sample, this is mostly relevant for δ Scuti stars (Gautschy & Saio 1996; Breger 2000), of which there are 360 in the ASCC-VSX cross matched catalogue. At long periods (> 10 days), two main causes for the relatively low recovery rate (425/623 = 68%) can be identified. Firstly, since the MASCARA data set spans 424 days, stars with long periods simply have fewer cycles in the data. This reduces the robustness against missing or bad data and instrumental effects, such as that caused by the moon. Secondly, many long-period variables also show multi-periodicity and irregularities in the shapes, amplitudes and periods of their light curves (Nicholls et al. 2009; Tabur et al. 2009; Spano et al. 2011; Bányai et al. 2013), which both make it more difficult to determine the main period over only a few cycles, and can cause the current period of the star to be inherently different from that measured previously. When searching for new unknown variable stars in the MASCARA data, as discussed below, the dependence of the recovery rate on amplitude and period has implications on the reliability of the parameters found.

Table 1. Eclipsing binaries in the MASCARA sample that exhibit the O'Connell effect. Periods include a 3σ confidence interval. The amplitude is that of the full oscillation in the MASCARA band. Δm is the difference in magnitude between the primary (after primary minimum) and secondary (before primary minimum) maxima in the binned light curve. No previous detections of the O'Connell effect in HD 219561 and V1392 Ori were found.

ASCC	Identifier	V	RA (J2000)	Dec (J2000)	Period (days)	Amplitude (mag)	Δm (mmag)	Previous detection
307947	V376 And	7.77	$02^h35'11.6''$	$+49°51'37''$	0.79867(6)	0.29	44	(1)
449928	HD 219561[a]	8.40	$23^h16'21.2''$	$+41°33'43''$	0.56660(5)	0.28	21	–
513514	V556 Lyr	8.14	$19^h25'08.3''$	$+35°59'58''$	1.4901(3)	0.13	13	(2)
521078	V448 Cyg	8.14	$20^h06'09.9''$	$+35°23'10''$	6.519(2)	0.37	18	(3)
558695	V600 Per	7.86	$03^h19'01.4''$	$+32°41'16''$	1.4697(1)	0.39	26	(4)
725559	ER Vul	7.35	$21^h02'25.9''$	$+27°48'26''$	0.69810(5)	0.13	13	(5)
1017908	V1392 Ori	7.76	$06^h16'17.9''$	$+09°01'40''$	1.3881(1)	0.20	24	–

Notes. [(a)] Identified as NSVS 6156390 in the ASCC-VSX cross-match; identified as TYC 3225-1270-1 in the ASCC catalogue.

References. (1) Djurašević et al. (2008); (2) Hartman et al. (2004); (3) Djurašević et al. (2009); (4) Campos-Cucarella et al. (1997); (5) Olah et al. (1994).

From the whole test sample of 2776 known variables, 401 (14.4%) are not recovered. Of these, 98 are classified in the VSX as irregular or semi-regular; the non-recovery of these stars can be explained intuitively by irregularities in their behaviour. A further 47 stars belong to classes of variable stars known to show multi-periodicity, which also easily explains their non-recovery. This leaves 256 stars of which the non-recovery cannot be easily explained by their class. For 69 of these, no variability larger than the typical scatter in the binned data points (0.03 magnitude) is detected. Additionally some cases of non-recovery can be explained by outliers in the data, aliasing, or incomplete filtering of either of the two systematics described in Sect. 3.2. Finally there are some examples of which the light curve appears to be well-described by the found period; these may be cases of previously unknown multi-periodicity, periods that have changed over time, or simply errors in the VSX catalogue. A more thorough analysis of the unrecovered known variables would be needed to assign individual stars to each of these classes.

The MASCARA data can also effectively be used to further characterise known variable stars. For example, for 210 stars the MASCARA data determines for the first time a period. By detecting the O'Connell effect in several eclipsing binaries, we show that MASCARA data are of sufficient quality to study second order variability effects in the brightest stars in the sky.

As presented in Sects. 4.2 and 4.3, we have determined new parameters for 210 known variables from the VSX catalogue, shown in Table A.1 in Appendix A, and identified 282 new candidate variable stars, which are presented in Table B.1 in Appendix B. We note that this only means that these stars either are not present in the VSX catalogue, or are present but lack parameters, and that some may already have been recorded in the extended literature. Although the new candidates have been vetted for possible known background variable stars in the VSX database that could cause the observed variability, they need to be observed with camera systems with significantly smaller pixel scales to exclude the contribution from possible faint unknown variable stars within the 2.5′ aperture used for the MASCARA photometry and beyond.

The recovery rate discussed in Sect. 4.1 and its dependence on the period of variability are important to take into account. For stars with periods < 0.1 and $\gtrsim 10$ days, the recovery rate of known variables is as low as 68%, casting doubt on the accuracy of the parameters determined with MASCARA for such stars. However, there are also mismatches between VSX and ASCC that are not only due to issues with the data or analysis. For example, there are stars that have multiple periods or irregular variability. Follow-up, either with more MASCARA data or with different instruments, can clear up the accuracy of the new parameters.

We note that our methods are sensitive to periodic variable stars, not to non-periodic ones. An alternative analysis, for instance a comparison with nearby stars, may be suited to find and characterise such stars. Additionally, the analysis is only performed on known stars in the ASCC master catalogue. This means that such objects as novae and flare stars, which were faint when the catalogue was created but can reach MASCARA magnitudes at later times, will not be detected with our analysis.

One interesting question that remains is why some of the new candidates have not previously been seen to be variable. For instance, ASCC 201832 (TYC 3926-224-1) has a V-magnitude of 7.42, a period of 0.61747(5) days and an amplitude of 160 mmag. Its light curve, given in Fig. 7, shows a very clear and regular variability, and one could reasonably expect this variable star to have been noticed earlier. A possible explanation for this lack of previous detection, as discussed in Sect. 1, is the fact that many previous surveys have focused on fainter stars than MASCARA and thus these stars may simply have 'slipped through'. Additionally, many of the new variables have very short (< 0.1 days) or very long (> 10 days) periods. Previous studies may not have had the cadence or duration necessary to detect such variability.

Acknowledgements. This project has received funding from the European Research Council (ERC) under the European Union's Horizon 2020 research and innovation programme (grant agreement nr. 694513).

References

Anderson, R. I., Saio, H., Ekström, S., Georgy, C., & Meynet, G. 2016, A&A, 591, A8
Bányai, E., Kiss, L. L., Bedding, T. R., et al. 2013, MNRAS, 436, 1576
Breger, M. 2000, in Astronomical Society of the Pacific Conference Series, Vol. 210, Delta Scuti and Related Stars, ed. M. Breger & M. Montgomery, 3
Campos-Cucarella, F., Gomez-Forrellad, J. M., & Garcia-Melendo, E. 1997, Information Bulletin on Variable Stars, 4426
Djurašević, G., Vince, I., Khruzina, T. S., & Rovithis-Livaniou, E. 2009, MNRAS, 396, 1553
Djurašević, G., Ekmekçi, F., Albayrak, B., Selam, S. O., & Erkapic, S. 2008, Rev. Mexicana Astron. Astrofis., 44, 249
ESA, ed. 1997, ESA Special Publication, Vol. 1200, The HIPPARCOS and TYCHO catalogues. Astrometric and photometric star catalogues derived from the ESA HIPPARCOS Space Astrometry Mission

Fabricius, C., Høg, E., Makarov, V. V., et al. 2002, A&A, 384, 180
Gaia Collaboration, Brown, A. G. A., Vallenari, A., et al. 2018, ArXiv e-prints [arXiv:1804.09365]
Gaia Collaboration, Brown, A. G. A., Vallenari, A., et al. 2016, A&A, 595, A2
Gautschy, A. & Saio, H. 1996, ARA&A, 34, 551
Groenewegen, M. A. T. & Jurkovic, M. I. 2017, A&A, 603, A70
Hartman, J. D., Bakos, G., Stanek, K. Z., & Noyes, R. W. 2004, AJ, 128, 1761
Holl, B., Audard, M., Nienartowicz, K., et al. 2018, ArXiv e-prints [arXiv:1804.09373]
Hubble, E. 1929, Proceedings of the National Academy of Science, 15, 168
Jetsu, L., Porceddu, S., Lyytinen, J., et al. 2013, ApJ, 773, 1
Kharchenko, N. V. 2001, Kinematika i Fizika Nebesnykh Tel, 17, 409
Malkov, O. Y., Tamazian, V. S., Docobo, J. A., & Chulkov, D. A. 2012, A&A, 546
Nicholls, C. P., Wood, P. R., Cioni, M.-R. L., & Soszyński, I. 2009, MNRAS, 399, 2063
O'Connell, D. J. K. 1951, Publications of the Riverview College Observatory, 2, 85
Olah, K., Budding, E., Kim, H.-L., & Etzel, P. B. 1994, A&A, 291, 110
Pepper, J., Pogge, R. W., DePoy, D. L., et al. 2007, PASP, 119, 923
Pojmański, G. 2002, Acta Astron., 52, 397
Pourbaix, D., Tokovinin, A. A., Batten, A. H., et al. 2004, A&A, 424, 727
Pribulla, T., Rucinski, S., Matthews, J. M., et al. 2008, MNRAS, 391, 343
Prša, A., Batalha, N., Slawson, R. W., et al. 2011, AJ, 141, 83
Ricker, G. R., Winn, J. N., Vanderspek, R., et al. 2015, Journal of Astronomical Telescopes, Instruments, and Systems, 1, 014003
Scargle, J. D. 1982, ApJ, 263, 835
Smolec, R. 2016, MNRAS, 456, 3475
Soszyński, I., Poleski, R., Udalski, A., et al. 2008, Acta Astron., 58, 163
Spano, M., Mowlavi, N., Eyer, L., et al. 2011, A&A, 536, A60
Tabur, V., Bedding, T. R., Kiss, L. L., et al. 2009, MNRAS, 400, 1945
Talens, G. J. J., Albrecht, S., Spronck, J. F. P., et al. 2017a, A&A, 606, A73
Talens, G. J. J., Justesen, A. B., Albrecht, S., et al. 2017b, ArXiv e-prints [arXiv:1707.01500]
Talens, G. J. J., Spronck, J. F. P., Lesage, A.-L., et al. 2017c, A&A, 601, A11
Torres, G., Andersen, J., & Giménez, A. 2010, A&A Rev., 18, 67
Udalski, A., Szymański, M. K., & Szymański, G. 2015, Acta Astron., 65, 1
Weiss, W. W., Rucinski, S. M., Moffat, A. F. J., et al. 2014, PASP, 126, 573
Wilsey, N. J. & Beaky, M. M. 2009, Society for Astronomical Sciences Annual Symposium, 28, 107
Zechmeister, M. & Kürster, M. 2009, A&A, 496, 577

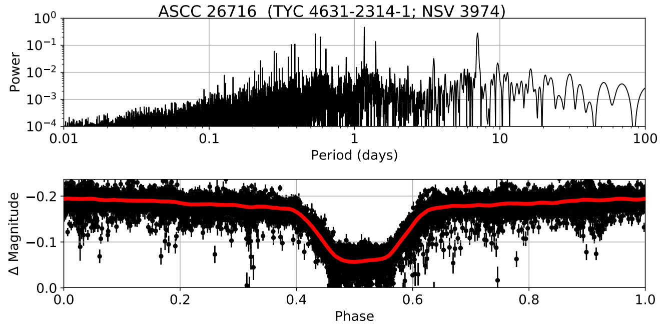

Fig. A.1. ASCC 26716 (TYC 4631-2314-1; NSV 3974); p = 1.1664(2) d.

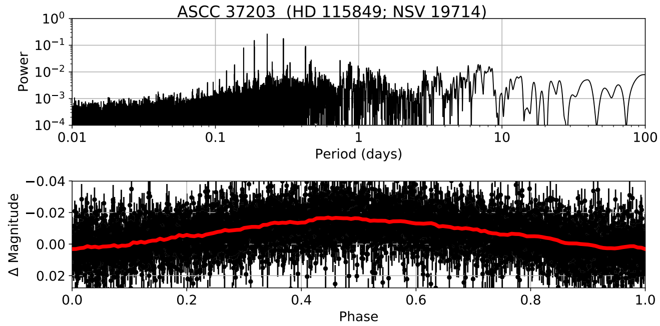

Fig. A.2. ASCC 37203 (HD 115849; NSV 19714); p = 0.2297(2) d.

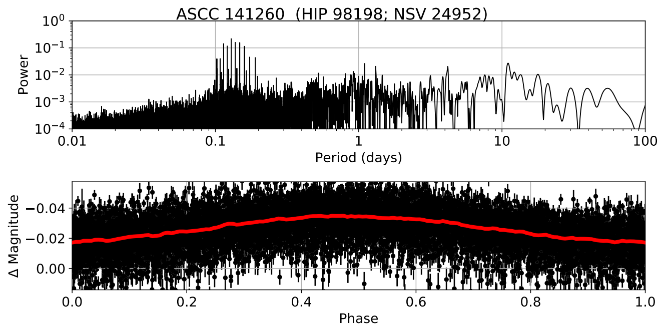

Fig. A.3. ASCC 141260 (HIP 98198; NSV 24952); p = 0.12879(4) d.

Appendix A: New parameters of known and suspected variables

The GLS periodograms (top panel) and phase folded light curves (bottom panel) of seven example known variable stars with new parameters from MASCARA are provided here. These figures can be found for all 210 such stars at `https://home.strw.leidenuniv.nl/~burggraaff/MASCARA_variables/`.

Notes for Table A.1.

[a] Variability types in the 'MASCARA' column were visually estimated based on the shape, period and amplitude of the light curve. These are only included if they disagree with or complement the VSX catalogue. 'E' indicates an eclipsing binary, 'P' a pulsating variable.

[b] Errors correspond to a 3σ confidence interval. For entries marked with a colon (:), no such confidence interval could be determined – these are listed with two significant digits.

[c] Amplitude in the MASCARA band.

[d] Epoch of a minimum in brightness.

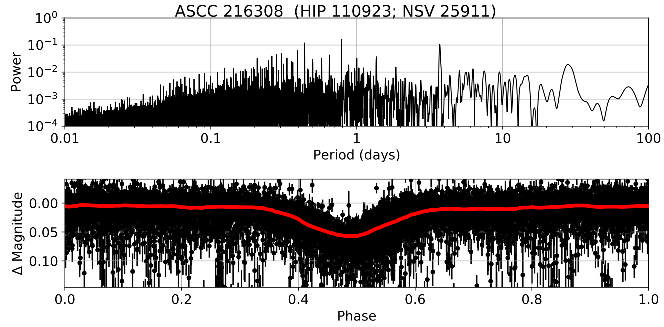

Fig. A.4. ASCC 216308 (HIP 110923; NSV 25911); p = 0.7866(6) d.

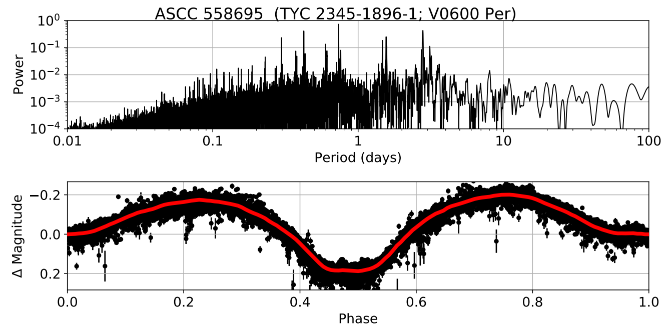

Fig. A.5. ASCC 558695 (TYC 2345-1896-1; V0600 Per); p = 1.4697(1) d.

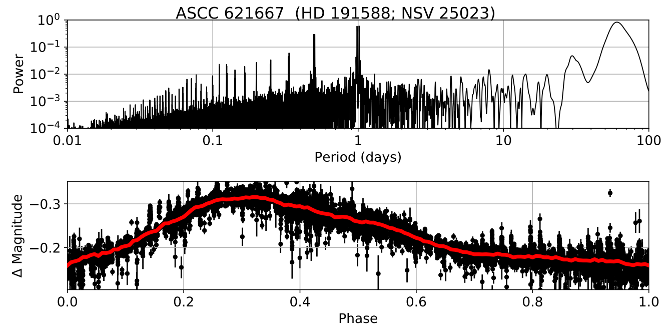

Fig. A.6. ASCC 621667 (HD 191588; NSV 25023); p = 61(1) d.

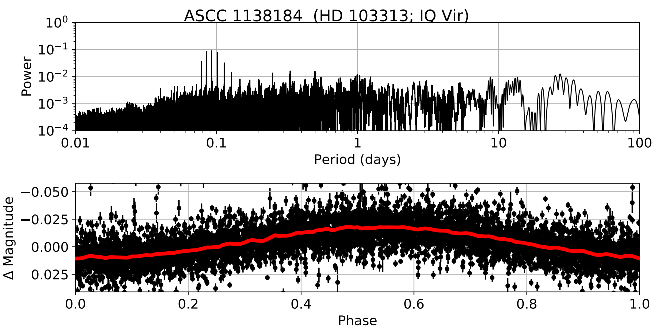

Fig. A.7. ASCC 1138184 (HD 103313; IQ Vir); p = 0.092463(3) d.

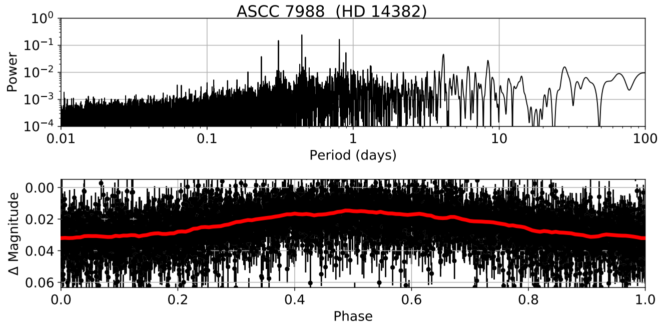

Fig. B.1. ASCC 7988 (HD 14382); p = 0.4457(8) d.

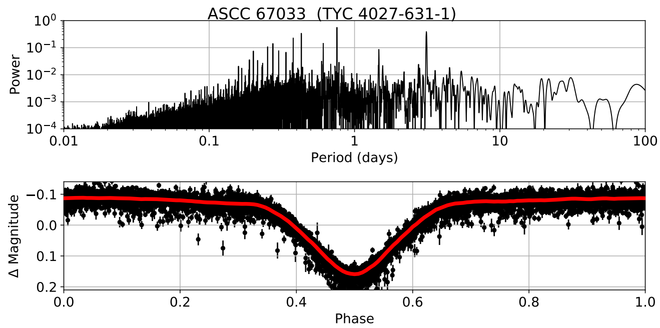

Fig. B.2. ASCC 67033 (TYC 4027-631-1); p = 0.7569(1) d.

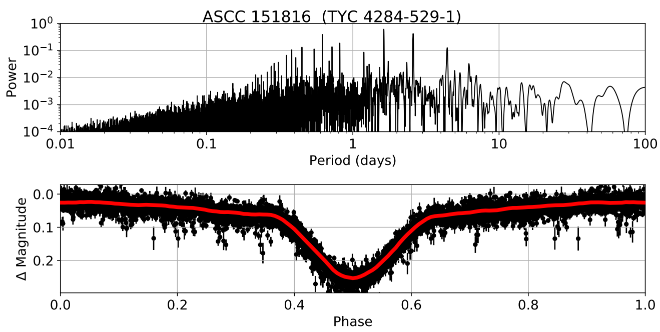

Fig. B.3. ASCC 151816 (TYC 4284-529-1); p = 1.6295(5) d.

Appendix B: New variable star candidates

The GLS periodograms (top panel) and phase folded light curves (bottom panel) of seven example candidate new variable stars from MASCARA are provided here. These figures can be found for all 282 such stars at `https://home.strw.leidenuniv.nl/~burggraaff/MASCARA_variables/`.

Notes for Table B.1.
[a] Variability types were visually estimated based on the shape, period and amplitude of the light curve. 'E' indicates an eclipsing binary, 'P' a pulsating variable.
[b] Errors correspond to a 3σ confidence interval. For entries marked with a colon (:), no such confidence interval could be determined – these are listed with two significant digits.
[c] Amplitude in the MASCARA band.
[d] Epoch of a minimum in brightness.

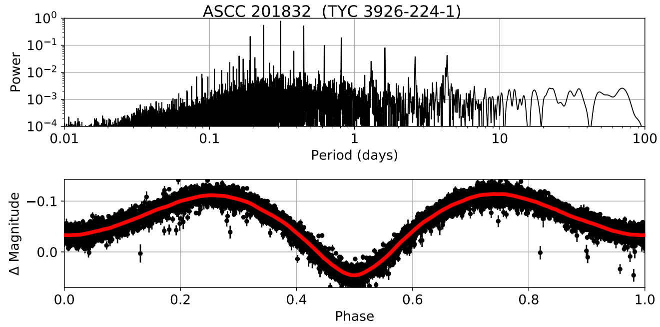

Fig. B.4. ASCC 201832 (TYC 3926-224-1); p = 0.61747(6) d.

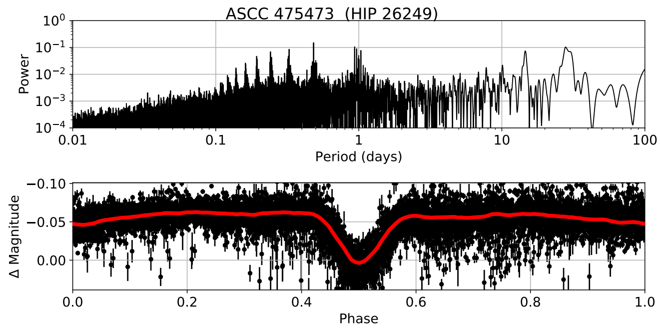

Fig. B.5. ASCC 475473 (HIP 26249); p = 0.9656(2) d.

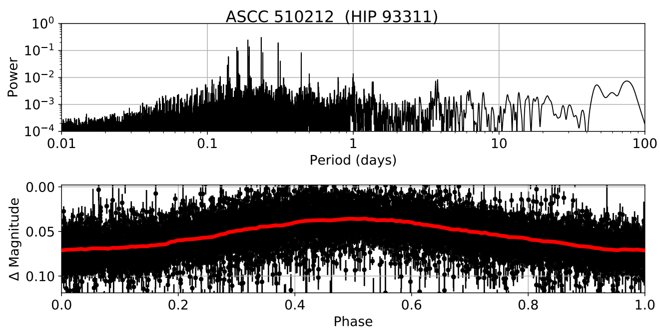

Fig. B.6. ASCC 510212 (HIP 93311); p = 0.23392(6) d.

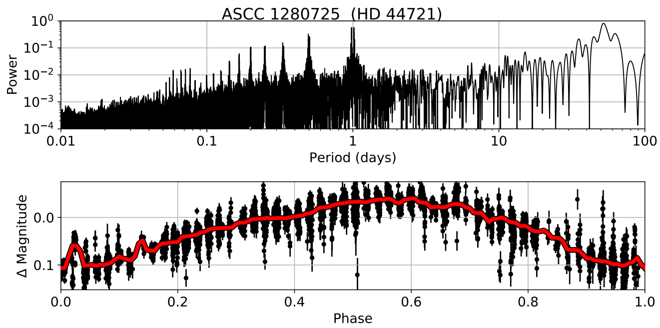

Fig. B.7. ASCC 1280725 (HD 44721); p = 52.0(7) d.

Table A.1. Known and suspected variable stars from the VSX catalogue without well-determined parameters (period and amplitude) detected with MASCARA.
The full version of this table is also available in electronic form at the CDS via anonymous ftp to cdsarc.u-strasbg.fr (130.79.128.5) or via `http://cdsweb.u-strasbg.fr/cgi-bin/qcat?J/A+A/`.

ASCC	Identifier	VSX ID	Var. Type[a]		V	RA (J2000)	Dec (J2000)	Nr. Obs.	Period[b]	Amp.[c]	Epoch[d]
			VSX	MASCARA					(days)	(mmag)	(HJD −2 450 000)
7 027	HIP 9494	V0779 Cas	EA:	–	6.69	$02^h02'09.3''$	$+75°30'08''$	8857	6.3530(7)	263	7203.5844
7 512	HIP 10309	NSV 15448	DSCTC:	–	6.45	$02^h12'49.9''$	$+79°41'30''$	9574	0.21:	7	7227.72
11 321	HD 21179	V0805 Cas	SRB	–	6.39	$03^h30'19.4''$	$+71°51'50''$	7274	39.4(1)	110	7240.7
18 914	HIP 26940	NSV 16615	–	P	6.77	$05^h43'00.7''$	$+73°59'09''$	5912	0.088:	48	7201.718
22 011	HD 47505	EP Cam	SRB	–	8.07	$06^h48'37.5''$	$+76°59'24''$	6223	39.6(1)	194	7234.7
22 755	HIP 34101	CM Cam	FKCOM	–	6.99	$07^h04'15.1''$	$+75°24'41''$	5541	15.87(6)	65	7377.4
24 395	HIP 36978	NSV 17498	–	–	7.73	$07^h36'02.2''$	$+76°50'00''$	6165	23.1(4)	58	7306.7
26 716	TYC 4631-2314-1	NSV 3974	–	E	8.31	$08^h25'12.0''$	$+84°00'51''$	11785	1.1664(2)	139	7280.4131
27 874	HD 74225	FL Cam	LB	–	7.01	$08^h50'46.6''$	$+78°09'55''$	5776	35.68(5)	207	7219.38
31 460	HIP 51111	NSV 18397	–	–	8.29	$10^h26'33.2''$	$+73°47'16''$	5616	22.2(4)	79	7192.4
33 669	HIP 56328	FP Cam	LB:	–	8.17	$11^h32'52.4''$	$+79°54'60''$	6567	44:	123	7329
34 601	HD 104216	FR Cam	LB	–	6.21	$12^h00'18.6''$	$+80°51'11''$	8097	78.0(7)	149	7273.4
37 203	HD 115849	NSV 19714	–	P	7.78	$13^h17'37.4''$	$+71°14'48''$	7136	0.2297(2)	20	7136.7374
40 687	HD 132770	TT UMi	SRB	–	6.91	$14^h55'00.2''$	$+74°52'52''$	8390	25.1(2)	108	7375.7
47 075	HD 160538	DR Dra	RS	–	6.62	$17^h32'41.2''$	$+74°13'38''$	9965	26.74(4)	82	7153.51
59 205	HIP 108034	NSV 25787	–	E	6.99	$21^h53'11.9''$	$+71°59'23''$	10479	1.5970(8)	74	7218.5899
60 871	HD 213571	NSV 25918	VAR:	–	7.15	$22^h30'00.3''$	$+70°10'17''$	10379	1.229(3)	22	7272.359
63 952	HD 220140	V0368 Cep	RS	–	7.53	$23^h19'26.6''$	$+79°00'13''$	11035	2.709(4)	69	7294.706
66 481	HD 225136	V0398 Cep	SRB	–	6.34	$00^h03'51.6''$	$+66°42'44''$	9003	22.04(3)	81	7152.67
66 708	HIP 957	NSV 15045	VAR:	–	7.38	$00^h11'50.5''$	$+66°07'35''$	9071	1.434(2)	31	7173.724
81 185	HD 93238	GY UMa	SRB	–	7.0	$10^h47'36.7''$	$+65°36'60''$	5339	20.54(2)	104	7163.52
81 872	HD 100029	NSV 5231	SR	–	3.81	$11^h31'24.2''$	$+69°19'52''$	3263	0.9366(5)	34	7220.4158
85 336	HD 135119	NSV 20266	–	P	7.12	$15^h09'06.2''$	$+69°39'11''$	8349	0.09514(2)	14	7229.53321
85 978	HD 141060	FW Dra	LB	–	7.89	$15^h42'41.9''$	$+67°03'60''$	8916	17.1(3)	60	7179.5
93 108	HD 194258	AC Dra	LB	–	5.68	$20^h20'06.0''$	$+68°52'49''$	10658	37:	125	7058
96 253	HD 208682	NSV 13966	–	–	5.97	$21^h55'31.0''$	$+65°19'15''$	10253	0.733(1)	14	7230.591
109 220	HD 11401	NSV 647	–	–	7.92	$01^h54'00.5''$	$+60°09'11''$	7640	38.3(4)	191	7244.5
111 649	HD 15727	NSV 15547	–	–	8.24	$02^h34'36.2''$	$+64°47'21''$	7467	0.6307(7)	38	7323.7284
122 362	HD 49671	BR Lyn	SRB:	–	8.0	$06^h53'38.1''$	$+61°00'56''$	4393	83.2(3)	245	7309.6
123 887	HIP 37595	FG Cam	SRD	–	7.88	$07^h42'50.5''$	$+61°09'27''$	4264	34.1(3)	126	7436.4
127 333	HD 89546	FG UMa	RS	–	7.4	$10^h21'47.5''$	$+60°54'46''$	4918	21.7(1)	127	7208.4
128 738	HD 100933	NSV 18812	–	–	7.38	$11^h37'24.6''$	$+62°11'47''$	5046	19.45(8)	113	7165.44
131 523	HD 127411	IT Dra	DSCTC	–	7.52	$14^h28'58.0''$	$+60°23'11''$	8632	0.059:	14	7169.57
131 579	HD 127929	ER Dra	DSCTC	–	6.26	$14^h31'42.8''$	$+60°13'32''$	8635	0.0879(7)	10	7228.4029
141 260	HIP 98198	NSV 24952	VAR:	P	7.49	$19^h57'16.0''$	$+62°52'36''$	9884	0.12879(4)	18	7200.65832
143 767	HD 198781	NSV 25362	–	–	6.45	$20^h49'17.4''$	$+64°02'32''$	9589	0.651(1)	15	7234.699
147 038	HD 209145	V0439 Cep	BE:	–	7.66	$21^h59'19.7''$	$+60°17'52''$	10732	0.7973(8)	38	7161.6815
148 893	HIP 111379	HD 214007	E	–	6.54	$22^h33'53.1''$	$+61°46'41''$	9438	20.34(2)	78	7227.42
150 393	HD 218537	NSV 26026	–	–	6.25	$23^h07'47.7''$	$+63°38'00''$	9621	0.76:	6	7214.62

Table A.1. Continued.

ASCC	Identifier	VSX ID	Var. Type[a] VSX	Var. Type[a] MASCARA	V	RA (J2000)	Dec (J2000)	Nr. Obs.	Period[b] (days)	Amp.[c] (mmag)	Epoch[d] (HJD −2 450 000)
152 675	HD 222670	V0816 Cas	LB	–	6.58	23^{h}42′21.0″	+64°30′55″	8760	39.0(4)	83	7300.4
167 549	HD 12709	NSV 15438	VAR:	E	7.98	02^{h}06′16.4″	+57°18′26″	7871	6.33(3)	59	7273.7
169 557	HD 14489	V0474 Per	ACYG	–	5.2	02^{h}22′21.4″	+55°50′44″	8085	0.9795(7)	29	7204.7105
174 279	HD 22298	CT Cam	BE	–	7.69	03^{h}38′01.0″	+55°10′15″	7502	5.27(5)	42	7300.52
174 987	HD 24395	NSV 15840	–	P	6.91	03^{h}55′46.4″	+56°55′08″	5855	0.24065(9)	25	7347.51248
181 744	HD 43979	NSV 16836	–	P	7.52	06^{h}22′26.0″	+56°00′47″	6088	0.1079(3)	19	7377.5379
185 810	HIP 39348	AE Lyn	RS	–	6.49	08^{h}02′35.8″	+57°16′25″	4694	10.10(8)	29	7286.75
195 452	HD 136617	FS Dra	LB	–	8.21	15^{h}18′47.5″	+59°31′17″	9145	32(1)	102	7463
197 581	HD 151199	NSV 7945	–	–	6.17	16^{h}42′58.5″	+55°41′24″	11860	2.226(9)	14	7206.413
201 778	HD 173605	NSV 24573	–	–	7.94	18^{h}42′49.5″	+57°51′55″	11163	3.63(3)	37	7219.51
205 426	HIP 96989	V2089 Cyg	SRB	–	8.26	19^{h}42′49.3″	+55°01′37″	12991	22.8(3)	84	7134.7
206 937	HD 190397	V2104 Cyg	IA	P	7.69	20^{h}01′45.5″	+57°39′07″	11907	0.2121(1)	15	7262.5718
210 621	HIP 104605	NSV 25514	–	E	7.92	21^{h}11′24.2″	+57°37′13″	11270	0.803(1)	27	7216.545
212 098	HD 206267	NSV 25719	VAR	–	5.7	21^{h}38′57.6″	+57°29′21″	11784	1.856(5)	16	7292.539
212 342	HD 206773	NSV 25749	–	–	6.92	21^{h}42′24.2″	+57°44′10″	11701	0.3702(6)	12	7304.506
213 011	HD 208095	NSV 13909	BCEP:	–	5.68	21^{h}52′01.0″	+55°47′48″	11931	2.91(1)	19	7272.66
216 308	HIP 110923	NSV 25911	–	E	8.28	22^{h}28′24.0″	+57°39′43″	11364	0.7866(6)	54	7178.6907
217 340	HD 214665	V0416 Lac	LB	–	5.18	22^{h}38′37.9″	+56°47′44″	11663	35.37(4)	165	7281.72
222 088	HIP 115368	V0813 Cas	BE	–	7.93	23^{h}22′10.5″	+56°20′54″	10838	0.2956(2)	33	7404.3374
244 177	HD 29317	NSV 1681	RS:	–	5.07	04^{h}39′54.7″	+53°04′46″	9557	0.16(5)	8	7390.38
259 732	HD 126138	HD 126138	VAR	P	7.54	14^{h}21′59.9″	+53°31′16″	13718	0.18:	11	7185.44
260 157	HD 129779	EH Boo	LB:	–	7.52	14^{h}42′23.2″	+54°48′12″	11625	87.4(3)	182	7058.8
272 564	HD 189859	V2101 Cyg	LB	–	7.22	19^{h}59′53.8″	+52°08′59″	16690	76:	248	7221
273 385	HD 192034	V2112 Cyg	LB	–	7.48	20^{h}10′32.9″	+52°23′06″	16473	41:	146	7269
276 817	HD 198624	NSV 25356	VAR:	–	6.6	20^{h}49′37.7″	+50°07′38″	17522	64.9(1)	155	7169.6
297 672	HD 1240	NSV 15065	VAR:	–	6.53	00^{h}16′54.0″	+49°27′43″	14012	41:	80	7185
303 910	HIP 7919	NSV 15362	–	E	7.89	01^{h}41′46.7″	+49°18′12″	10980	7.029(6)	176	7281.577
312 027	HD 22136	NSV 1197	–	–	6.87	03^{h}35′58.5″	+47°05′28″	12282	0.9312(9)	23	7380.4703
313 455	HIP 18838	NSV 15867	–	E	7.91	04^{h}02′20.3″	+47°30′24″	11835	1.619(1)	54	7342.353
313 502	HD 25293	NSV 15871	–	E	6.96	04^{h}03′22.1″	+48°50′27″	11645	2.888(2)	57	7237.695
317 993	HD 36719	NSV 16379	–	P	6.1	05^{h}36′16.0″	+47°42′55″	9904	0.086961(6)	18	7348.772115
323 009	HIP 36056	NSV 17459	–	E	6.77	07^{h}25′52.0″	+48°32′52″	10591	4.951(3)	38	7271.738
339 426	HD 168269	NSV 24367	–	–	7.47	18^{h}16′24.9″	+48°22′08″	17150	20.43(9)	98	7210.6
341 219	HD 174637	V0538 Lyr	LB	–	7.65	18^{h}49′07.9″	+47°30′57″	16915	35.06(2)	271	7067.79
367 065	HD 217050	EW Lac	GCAS	–	5.33	22^{h}57′04.5″	+48°41′03″	15727	0.36171(9)	31	7218.59859
389 991	HIP 19647	V0584 Per	GCAS	–	8.01	04^{h}12′36.5″	+42°07′06″	9360	0.7601(9)	25	7322.5621
408 126	HD 100018	NSV 18777	–	E	6.82	11^{h}30′49.9″	+41°17′12″	10595	7.399(3)	50	7083.624
408 281	HD 101207	NSV 5279	–	E	7.9	11^{h}38′57.2″	+41°08′35″	10620	1.09014(6)	104	7068.61596
412 871	HD 135530	NSV 20281	VAR:	–	6.14	15^{h}14′10.3″	+42°10′17″	13922	20.04(8)	65	7204.42
420 256	HD 169746	V0528 Lyr	SRB	–	6.63	18^{h}23′60.0″	+43°54′28″	15427	24.70(3)	67	7143.63
422 429	HD 175404	V0541 Lyr	LB	–	6.71	18^{h}53′18.5″	+40°59′43″	13395	33.21(3)	119	7152.64

Table A.1. Continued.

ASCC	Identifier	VSX ID	Var. Type[a] VSX	MASCARA	V	RA (J2000)	Dec (J2000)	Nr. Obs.	Period[b] (days)	Amp.[c] (mmag)	Epoch[d] (HJD −2 450 000)
444 150	HD 209515	V1942 Cyg	ACV	–	5.61	22^{h}02′56.7″	+44°38′60″	13580	2.388(8)	24	7385.333
448 014	HIP 112707	NSV 25964	–	E	8.02	22^{h}49′28.4″	+43°50′37″	14091	5.051(5)	69	7192.679
448 900	HD 217675	omi And	GCAS	–	3.63	23^{h}01′55.3″	+42°19′34″	10383	1.5635(7)	57	7264.6126
450 133	HIP 115134	NSV 26060	–	P	8.13	23^{h}19′14.0″	+40°07′16″	10344	0.050855(5)	32	7291.402983
450 172	TYC 3225-18-1	HD 219980	VAR	P	7.57	23^{h}19′52.5″	+42°57′49″	12110	0.7688(6)	34	7237.5813
450 476	HD 220524	V0385 And	LB	–	6.41	23^{h}24′08.9″	+41°36′46″	12422	35.6(1)	96	7323.4
464 151	HIP 12465	AH Tri	SRD	–	8.3	02^{h}40′31.3″	+36°00′21″	10030	36.1(7)	125	7475.4
467 588	HD 21856	NSV 15713	–	P	5.9	03^{h}32′40.0″	+35°27′42″	10295	0.058663(4)	15	7389.360438
474 018	HD 34921	V0420 Aur	HMXB:+GCAS	–	7.44	05^{h}22′35.2″	+37°40′34″	9333	0.6736(3)	39	7277.5768
487 067	HIP 40931	CT Lyn	SRB	–	8.06	08^{h}21′11.3″	+35°19′48″	8976	38.5(1)	187	7349.8
489 310	HD 80492	NSV 18175	RS	–	6.65	09^{h}21′15.5″	+39°39′59″	10833	24.3(2)	62	7384.5
492 628	HD 99002	CX UMa	DSCTC:	–	6.93	11^{h}23′53.3″	+37°14′05″	10321	0.063:	9	7405.693
504 249	HD 162208	NSV 23917	VAR:	P	7.6	17^{h}47′58.6″	+39°58′51″	13357	0.038121(2)	21	7108.62174
508 874	HIP 92282	NSV 24604	–	–	7.51	18^{h}48′28.1″	+36°26′27″	12092	1.427(2)	31	7240.6
511 086	HD 178475	iot Lyr	BE	–	5.25	19^{h}07′18.1″	+36°06′01″	11682	0.4658(3)	12	7435.76
520 545	HD 190466	NSV 24993	VAR:	–	7.19	20^{h}03′39.5″	+38°19′38″	12521	21.73(4)	89	7138.56
524 473	HD 194335	V2119 Cyg	BE	–	5.86	20^{h}23′44.4″	+37°28′35″	12159	0.4019(2)	21	7212.7278
525 210	TYC 3152-760-1	NSV 13103	–	–	7.6	20^{h}28′28.5″	+37°47′22″	12040	33.42(5)	132	7250.6
544 882	HIP 114305	V0381 And	EA	–	7.34	23^{h}08′57.1″	+38°54′55″	10256	21.82(1)	150	7197.53
545 570	HIP 115093	NSV 26058	–	P	7.36	23^{h}18′42.3″	+36°05′25″	10220	0.08719(2)	16	7343.39642
549 552	HD 2265	NSV 15092	–	–	7.54	00^{h}26′40.8″	+34°11′02″	10616	18.25(4)	108	7236.64
550 087	HD 3397	NSV 15136	–	P	7.64	00^{h}37′03.6″	+31°29′11″	10219	0.149(1)	15	7238.501
551 581	HIP 5148	NSV 15242	PULS	–	7.63	01^{h}05′54.2″	+32°59′37″	9847	0.15070(4)	24	7270.50392
558 695	TYC 2345-1896-1	V0600 Per	EB	–	7.86	03^{h}19′01.4″	+32°41′16″	9478	1.4697(1)	389	7388.5219
572 067	HD 45783	NSV 16879	SRB	–	7.46	06^{h}30′59.7″	+32°48′19″	8636	21.08(1)	156	7067.47
573 827	HD 49139	NSV 17192	–	P	8.13	06^{h}48′30.3″	+34°06′53″	9840	0.098542(7)	31	7386.506745
581 053	HD 74292	FL Cnc	DSCTC	–	7.03	08^{h}44′14.8″	+32°03′46″	9114	0.074599(4)	17	7430.633791
586 009	HD 98851	LR UMa	DSCTC:	–	7.41	11^{h}22′51.2″	+31°49′41″	10656	0.057:	13	7392.698
586 689	HD 103288	NSV 18997	DSCTC	–	7.0	11^{h}53′47.6″	+33°36′55″	9989	0.13745(1)	19	7124.46703
610 143	HIP 94862	V0555 Lyr	LB	–	8.34	19^{h}18′12.1″	+34°08′10″	12416	60(2)	81	7281
615 968	HD 186702	V2090 Cyg	SR	–	6.48	19^{h}44′38.2″	+34°24′51″	12089	79.7(6)	168	7118.7
621 667	HD 191588	NSV 25023	RS	–	8.24	20^{h}09′24.4″	+34°42′59″	11930	61(1)	157	7239
634 284	HIP 105813	NSV 25594	–	E	8.32	21^{h}25′47.8″	+33°28′56″	11308	2.930(2)	98	7135.734
638 991	HD 210514	PP Peg	LB	–	7.27	22^{h}10′17.0″	+32°17′17″	10774	26.85(2)	131	7194.64
643 373	HD 217241	NSV 25985	–	P	7.54	22^{h}58′59.0″	+34°04′01″	10175	0.047822(2)	42	7189.650662
644 172	HD 218742	V0345 Peg	SR	–	6.78	23^{h}10′08.9″	+33°46′04″	10222	62:	311	7167
650 545	HIP 5526	NSV 15251	–	P	8.09	01^{h}10′43.3″	+27°52′05″	9637	0.1944(7)	22	7294.691
654 939	HD 17382	BC Ari	BY	–	7.56	02^{h}48′09.1″	+27°04′07″	6245	0.062331(1)	105	7373.496831
655 972	HIP 15000	NSV 15650	–	P	8.3	03^{h}13′22.0″	+26°23′30″	8355	0.081152(8)	38	7302.502227
660 521	HD 33463	NSV 16257	–	–	6.43	05^{h}11′38.3″	+29°54′13″	8191	0.9467(8)	21	7228.714
663 529	HD 39478	NSV 16720	VAR:	P	8.25	05^{h}53′59.8″	+26°25′21″	8809	0.5478(2)	41	7253.6986

Table A.1. Continued.

ASCC	Identifier	VSX ID	Var. Type[a] VSX	Var. Type[a] MASCARA	V	RA (J2000)	Dec (J2000)	Nr. Obs.	Period[b] (days)	Amp.[c] (mmag)	Epoch[d] (HJD −2 450 000)
673 110	HD 57069	NSV 17433	VAR:	P	7.22	$07^h20'49.6''$	$+29°44'03''$	8470	0.21469(1)	42	7433.52136
679 969	HD 82191	NSV 4509	E	–	6.62	$09^h31'17.4''$	$+27°23'14''$	9831	9.016(4)	63	7064.481
681 478	HD 88639	NSV 18354	–	–	6.05	$10^h13'49.7''$	$+27°08'09''$	10036	58.0(5)	50	7423.8
693 946	HD 152877	NSV 20864	PULS	–	7.32	$16^h54'55.2''$	$+28°08'14''$	12293	0.07(5)	11	7202.47
699 494	HD 166181	V0815 Her	RS	–	7.69	$18^h08'16.0''$	$+29°41'28''$	12787	1.828(4)	40	7175.571
739 767	HD 784	NQ Peg	SRB	–	7.72	$00^h12'15.9''$	$+22°33'24''$	8902	69.8(2)	185	7330.4
745 883	HD 16629	AK Ari	LB:	–	7.94	$02^h40'31.7''$	$+21°11'16''$	8387	19.3(3)	78	7228.6
746 013	HD 17035	NSV 15568	–	P	8.2	$02^h44'45.1''$	$+24°11'04''$	8466	0.10726(1)	39	7370.49036
771 078	HD 72041	NSV 17909	–	P	5.69	$08^h31'30.5''$	$+24°04'52''$	9569	0.109096(7)	14	7057.481667
781 600	HD 124797	NSV 20071	PULS	–	6.77	$14^h15'01.6''$	$+23°41'10''$	11095	0.09750(3)	13	7099.71658
786 640	HD 150296	NSV 20729	–	–	7.53	$16^h39'17.4''$	$+22°13'16''$	11998	1.413(2)	39	7167.678
809 432	HD 192424	NSV 12927	–	E	7.36	$20^h14'04.5''$	$+22°13'25''$	11045	4.871(3)	78	7214.428
812 334	HIP 101263	NSV 25168	–	E	6.86	$20^h31'32.0''$	$+21°53'42''$	11282	9.666(6)	77	7247.557
823 625	HIP 110381	NSV 25882	–	E	7.68	$22^h21'26.8''$	$+21°02'53''$	9802	2.3602(5)	162	7223.6209
825 840	HD 216696	V0336 Peg	LB	–	7.48	$22^h54'40.4''$	$+24°23'14''$	10336	82.5(8)	161	7353.3
869 429	HD 120232	DL Boo	LB	–	7.58	$13^h47'57.4''$	$+18°56'40''$	10746	79.1(3)	160	7079.6
873 510	HIP 78409	HD 143551	VAR	P	7.93	$16^h00'23.6''$	$+15°40'03''$	11319	0.13146(2)	21	7142.59948
880 806	HD 164448	V0975 Her	LB	–	7.41	$18^h00'31.4''$	$+17°06'12''$	7786	88.2(2)	178	7303.4
888 109	HD 179588	V0338 Sge	E:	–	6.75	$19^h12'34.5''$	$+16°50'47''$	11427	3.499(2)	60	7265.399
895 793	HD 191178	V0344 Sge	LB	–	6.41	$20^h08'06.5''$	$+16°39'52''$	10545	76.1(3)	149	7094.7
904 796	HIP 106223	NSV 25635	–	P	8.36	$21^h30'57.0''$	$+16°34'16''$	10138	0.876(1)	55	7258.697
914 077	HIP 2559	HD 2912	PULS	–	8.38	$00^h32'31.3''$	$+10°29'12''$	10516	0.087:	19	7304.505
943 855	HIP 39837	NSV 17742	–	P	8.26	$08^h08'22.5''$	$+14°51'13''$	8388	0.9284(4)	52	7059.4835
949 562	HD 87271	GM Leo	DSCTC	–	7.14	$10^h04'08.4''$	$+11°37'43''$	10201	0.043988(6)	26	7431.520647
950 593	HD 91811	NSV 18447	–	–	8.14	$10^h36'21.8''$	$+14°47'37''$	7807	0.908(3)	31	7067.569
955 378	HD 115678	LQ Vir	LB	–	8.33	$13^h18'36.7''$	$+12°54'42''$	10223	86.9(7)	214	7165.4
963 519	HD 153415	V2359 Oph	LB	–	7.91	$16^h59'05.6''$	$+11°30'47''$	12241	22.73(5)	125	7474.71
965 614	HD 159736	NSV 22908	–	P	6.78	$17^h35'50.8''$	$+12°02'49''$	12013	0.9385(5)	37	7214.5799
974 753	HD 177175	V0915 Aql	LB	–	8.39	$19^h03'9.9''$	$+12°15'08''$	11790	83:	262	7200
976 482	HIP 95303	HD 182275	PULS	–	8.18	$19^h23'21.1''$	$+14°42'47''$	10549	0.06905(1)	25	7202.53897
976 799	HD 183144	NSV 12049	–	P	6.31	$19^h27'33.9''$	$+14°16'57''$	10518	0.3649(3)	10	7264.5498
987 551	HD 195922	NSV 25176	–	–	6.53	$20^h33'53.7''$	$+10°03'35''$	13726	0.13:	5	7326.36
994 510	HD 209288	NSV 14001	–	–	6.36	$22^h02'01.4''$	$+10°58'26''$	12534	4.29(5)	15	7271.64
997 489	HD 216930	V0337 Peg	LB	–	7.81	$22^h57'00.2''$	$+14°25'08''$	9359	23.21(5)	106	7262.43
1 002 291	HD 6266	HD 6266	DSCTC	–	7.74	$01^h03'40.7''$	$+05°14'07''$	8389	0.12220(4)	24	7341.54375
1 002 797	HD 8019	CV Psc	SRB	–	7.89	$01^h19'44.7''$	$+06°09'43''$	9737	23.0(2)	97	7398.4
1 006 099	HD 17986	EG Cet	SRB	–	6.66	$02^h53'46.2''$	$+09°20'09''$	10074	64.36(8)	194	7236.68
1 007 127	HIP 16120	NSV 15695	–	P	7.79	$03^h27'39.9''$	$+08°45'55''$	10022	0.063:	19	7251.726
1 019 675	HD 45530	V0648 Mon	ACV	–	7.48	$06^h28'14.0''$	$+05°16'20''$	10210	0.7919(4)	26	7094.4836
1 020 950	HD 47129	V0640 Mon	*	–	6.06	$06^h37'24.0''$	$+06°08'07''$	10439	0.60815(9)	34	7116.42173
1 027 427	HD 56031	NSV 3486	SR	–	5.83	$07^h15'39.4''$	$+07°58'40''$	11198	12.522(4)	88	7359.627

Table A.1. Continued.

ASCC	Identifier	VSX ID	Var. Type[a] VSX	MASCARA	V	RA (J2000)	Dec (J2000)	Nr. Obs.	Period[b] (days)	Amp.[c] (mmag)	Epoch[d] (HJD −2 450 000)
1 032 376	HD 65241	BU CMi	EA:	–	6.41	07^{h}58′05.9″	+07°12′49″	10774	2.9395(2)	155	7380.7921
1 045 080	HD 115521	NSV 6173	SR	–	4.79	13^{h}17′36.3″	+05°28′12″	12040	24.618(7)	109	7108.553
1 049 000	HIP 74471	OP Ser	LB:	–	8.31	15^{h}13′03.3″	+09°34′41″	13602	52.8(4)	236	7193.6
1 051 891	HIP 79539	HD 146026	VAR	P	7.41	16^{h}13′50.5″	+06°59′38″	13534	0.1752(1)	16	7182.498
1 058 727	HD 161223	V2314 Oph	DSCTC	–	7.44	17^{h}44′03.6″	+06°03′43″	13897	0.098051(8)	42	7221.572013
1 062 981	HD 168797	NW Ser	BE	–	6.14	18^{h}21′28.4″	+05°26′09″	14856	0.8433(6)	25	7168.5504
1 071 595	HD 183303	HD 183303	VAR	P	7.45	19^{h}28′35.9″	+08°51′49″	13553	0.13085(4)	22	7224.40561
1 078 861	HD 192873	V1481 Aql	LB	–	7.44	20^{h}17′00.3″	+07°04′18″	12166	34.70(8)	213	7211.72
1 088 003	HIP 109218	NSV 25836	VAR:	–	7.05	22^{h}07′31.4″	+09°40′16″	12947	0.617(1)	15	7263.517
1 092 522	HD 223637	HH Peg	SR	–	5.8	23^{h}51′21.2″	+09°18′48″	10626	21.03(2)	118	7430.33
1 093 676	HD 1586	BZ Psc	SRB:	–	7.56	00^{h}20′9.5″	+03°02′01″	6962	19.1(2)	84	7314.5
1 097 794	HD 13467	NSV 15455	ACV:	–	6.66	02^{h}11′43.4″	+03°27′10″	7831	0.29:	11	7331.58
1 102 248	HD 26691	V1138 Tau	SRB	–	8.19	04^{h}13′24.4″	+03°54′08″	8438	35.5(6)	119	7365.5
1 111 668	HD 44333	NSV 2932	ED	–	6.28	06^{h}21′25.8″	+02°16′07″	7110	5.564(1)	86	7340.619
1 138 184	HD 103313	IQ Vir	DSCTC	–	6.3	11^{h}53′50.3″	+00°33′08″	7790	0.092463(3)	29	7093.449967
1 150 768	HD 152468	HD 152468	PULS	–	7.56	16^{h}53′23.9″	+01°20′54″	9400	0.15195(2)	36	7221.49761
1 157 842	HD 167654	V2392 Oph	SRB	–	6.17	18^{h}16′05.6″	+02°22′39″	9063	25.76(3)	197	7202.65
1 168 837	HD 191029	NSV 25010	VAR:	P	7.15	20^{h}07′43.9″	+02°26′35″	8642	0.045:	9	7189.607
1 192 880	HD 25340	NSV 15869	VAR:	–	5.27	04^{h}01′32.0″	−01°32′59″	6575	0.8139(3)	30	7382.3871
1 195 268	HD 30637	HD 30637	VAR	–	7.16	04^{h}49′13.5″	−04°59′11″	5307	1.324(2)	32	7324.73
1 201 818	HD 43989	V1358 Ori	BY	–	7.95	06^{h}19′08.1″	−03°26′20″	7016	1.3592(7)	91	7348.7753
1 238 896	HD 147645	HD 147645	PULS	–	7.45	16^{h}23′05.9″	−00°51′22″	8640	0.15221(9)	18	7085.6775
1 255 441	HD 200139	IT Aqr	SR	–	7.32	21^{h}01′40.5″	−04°07′53″	7143	23.24(8)	216	7203.57
1 259 863	HD 211802	HD 211802	VAR	P	7.74	22^{h}19′49.0″	−04°03′59″	6761	0.040337(4)	30	7139.722185
1 263 973	HD 224639	BH Psc	DSCTC	–	7.13	23^{h}59′31.3″	−02°50′38″	6259	0.16086(4)	30	7268.65159
1 300 121	HD 71433	NSV 17893	VAR:	E	6.59	08^{h}27′17.3″	−06°24′35″	6650	2.257(1)	42	7131.46
1 304 804	HD 83047	NSV 18238	–	P	8.18	09^{h}35′37.3″	−08°35′20″	5303	0.096:	26	7126.435
1 307 417	HD 92243	NSV 18465	–	–	8.32	10^{h}38′50.6″	−08°13′29″	4062	0.49(2)	43	7477.37
1 335 735	HD 197451	NSV 25299	–	E	7.18	20^{h}43′57.0″	−05°35′25″	6626	1.803(5)	34	7286.442
1 338 228	HD 203540	IY Aqr	LB	–	7.86	21^{h}22′59.2″	−06°13′58″	5249	23.21(4)	127	7279.35
1 349 501	HD 17925	EP Eri	RS	–	6.04	02^{h}52′32.1″	-12°46′11″	2020	6.71(4)	42	7389.47
1 364 045	HD 49888	NSV 3231	–	–	7.17	06^{h}50′08.1″	-12°35′05″	3351	0.3446(5)	41	7332.7543
1 458 904	HD 62532	NSV 17574	–	–	8.38	07^{h}43′45.3″	-17°56′46″	2951	0.9001(5)	98	7414.4883
1 476 567	HD 97182	NSV 18688	–	P	8.06	11^{h}11′08.5″	-17°07′57″	3363	0.078:	27	7474.447
1 482 531	HD 120121	NSV 19964	–	–	7.48	13^{h}47′55.7″	-18°34′22″	3413	20.9(1)	149	7465.6
1 521 186	HD 2527	NSV 15099	–	–	7.13	00^{h}28′50.7″	-24°38′12″	2563	0.2131(2)	23	7344.4634
1 543 406	HD 52437	FU CMa	GCAS	–	6.52	07^{h}00′19.4″	-22°07′09″	3308	1.1093(5)	33	7369.6989
1 585 123	HD 138344	GG Lib	SR:	–	6.87	15^{h}32′15.1″	-23°52′49″	3729	35.65(3)	236	7095.75
1 598 287	HD 171369	V4190 Sgr	DSCTC	–	6.48	18^{h}35′21.3″	-20°50′26″	3146	0.09849(2)	27	7179.65807
1 619 379	HD 9692	BI Scl	LB:	–	6.89	01^{h}34′23.4″	-28°14′12″	1941	22.8(5)	116	7368.3
1 643 351	HD 59256	NSV 17483	–	–	5.55	07^{h}27′59.2″	-29°09′21″	3489	0.943(4)	17	7094.363

Table A.1. Continued.

ASCC	Identifier	VSX ID	Var. Type[a] VSX	Var. Type[a] MASCARA	V	RA (J2000)	Dec (J2000)	Nr. Obs.	Period[b] (days)	Amp.[c] (mmag)	Epoch[d] (HJD −2 450 000)
1 652 268	HD 66932	V0418 Pup	LB:	–	7.39	08^{h}04′38.8″	-29°57′58″	3253	21.47(8)	152	7071.45
1 660 685	HD 77339	AL Pyx	SR	–	7.21	09^{h}01′06.3″	-27°30′57″	3021	34.40(1)	272	7434.56
1 679 016	HD 129195	NSV 20159	–	E	7.0	14^{h}41′57.2″	-28°03′57″	3278	0.3778(6)	20	7143.6126
1 698 616	HD 173484	V4406 Sgr	SRB	–	6.91	18^{h}46′47.2″	-29°37′54″	3306	43.5(2)	193	7331.3
1 714 647	HD 2429	eta Scl	SR	–	4.87	00^{h}27′55.7″	-33°00′26″	1952	24.22(6)	260	7249.74
1 735 739	HD 59594	V0349 Pup	DSCTC	–	7.32	07^{h}29′17.1″	-34°10′17″	2666	0.048:	21	7082.403
1 811 651	HD 1721	NSV 15077	–	–	7.14	00^{h}21′14.7″	-35°47′56″	1263	19.3(3)	140	7385.3

Table B.1. New candidate variable stars detected with MASCARA.
The full version of this table is also available in electronic form at the CDS via anonymous ftp to cdsarc.u-strasbg.fr (130.79.128.5) or via `http://cdsweb.u-strasbg.fr/cgi-bin/qcat?J/A+A/`

ASCC	Identifier	Var. Type[a]	V	RA (J2000)	Dec (J2000)	Nr. Obs.	Period[b] (days)	Amp.[c] (mmag)	Epoch[d] (HJD −2 450 000)
3 132	HIP 4090	–	7.72	00^{h}52′29.0″	+79°50′26″	10048	8.00(3)	52	7306.77
3 347	TYC 4619-1223-1	P	8.14	00^{h}56′10.8″	+85°27′33″	11238	0.094:	18	7292.544
7 335	TYC 4503-2063-1	P	7.0	02^{h}08′56.1″	+79°20′45″	9294	0.5414(7)	16	7279.5832
7 988	HD 14382	P	7.82	02^{h}23′04.7″	+70°20′36″	7800	0.4457(8)	17	7279.6429
11 298	HD 20110	–	8.36	03^{h}29′50.9″	+84°02′20″	12276	33(1)	69	7212
20 609	TYC 4525-994-1	–	8.4	06^{h}17′55.6″	+76°40′29″	5497	82:	193	7269
23 934	HIP 36159	E	7.38	07^{h}26′57.6″	+75°36′44″	5942	3.68(2)	24	7349.78
28 165	HD 75544	P	7.32	08^{h}58′22.7″	+78°08′45″	5446	0.11:	13	7153.37
42 606	HIP 77211	P	8.16	15^{h}45′53.1″	+82°22′12″	10754	0.57:	19	7178.4
44 194	HD 149681	P	5.55	16^{h}25′43.5″	+78°57′49″	10229	0.05:	4	7192.457
45 290	HD 153845	P	7.35	16^{h}52′43.9″	+76°51′09″	10310	0.11:	9	7207.62
47 931	HIP 87385	P	6.74	17^{h}51′24.9″	+74°34′09″	10021	0.18954(7)	15	7323.43351
50 840	HIP 92431	P	7.86	18^{h}50′12.2″	+78°57′58″	11056	0.09353(3)	17	7256.70793
54 511	HD 190833	–	8.23	20^{h}01′34.0″	+70°27′16″	10684	0.56:	12	7230.66
56 687	HD 199019	–	8.2	20^{h}49′29.1″	+71°46′28″	10762	6.6(2)	31	7296.5
58 891	HD 208020	P	8.3	21^{h}46′09.2″	+80°42′35″	11815	0.086:	21	7132.731
59 137	HIP 107891	E	8.38	21^{h}51′35.3″	+71°53′08″	10475	0.86:	20	7346.4
59 793	TYC 4475-461-1	–	7.32	22^{h}07′21.2″	+74°43′59″	10812	37.8(2)	130	7161.7
62 747	HIP 113648	–	7.51	23^{h}01′01.0″	+76°07′21″	10697	47(3)	41	7336
65 569	TYC 4602-258-1	–	8.35	23^{h}47′23.2″	+75°16′53″	10187	16.5(2)	86	7262.7
65 605	HIP 117380	–	8.33	23^{h}47′59.5″	+80°33′54″	11106	1.5:	27	7229.6
67 033	TYC 4027-631-1	E	8.29	00^{h}23′36.8″	+66°12′45″	9029	0.7569(1)	248	7286.5364
71 546	TYC 4074-770-1	–	7.94	03^{h}32′06.6″	+66°18′08″	6521	42(3)	54	7235
75 478	TYC 4103-942-1	P	8.29	06^{h}05′59.4″	+65°09′19″	4121	0.081812(8)	50	7057.375742
77 786	HIP 37253	P	8.23	07^{h}39′02.6″	+67°03′01″	4565	0.18:	18	7375.63
77 978	HIP 37979	P	7.12	07^{h}47′04.9″	+69°09′17″	4726	0.079584(9)	17	7134.412389
80 987	HIP 51774	P	8.25	10^{h}34′46.7″	+68°51′49″	5437	0.06593(2)	28	7236.39016
82 644	HD 107379	E	7.11	12^{h}20′23.1″	+66°23′28″	6395	1.798(3)	36	7191.581
86 128	HIP 77612	E	8.2	15^{h}50′41.1″	+66°25′44″	8977	2.5:	18	7273.4
87 747	HIP 84047	P	7.62	17^{h}10′56.8″	+66°15′26″	9626	0.28:	12	7208.53
93 682	HIP 102224	–	7.01	20^{h}42′48.4″	+66°19′36″	10445	6.92(9)	21	7153.56
93 848	TYC 4460-432-1	–	7.99	20^{h}48′18.0″	+69°08′30″	10639	6.2(1)	24	7294.6
95 027	TYC 4257-1034-1	E	8.08	21^{h}25′57.4″	+65°15′41″	10309	2.113(1)	69	7131.737
95 086	HD 204770	–	5.41	21^{h}27′46.2″	+66°48′33″	10358	0.737(2)	9	7153.681
95 937	HD 207826	P	6.47	21^{h}49′08.1″	+66°47′32″	10320	1.363(6)	10	7193.492
100 947	HIP 526	P	7.97	00^{h}06′20.2″	+60°27′26″	8999	0.1070(7)	19	7219.6756
107 340	HD 9056	E	7.76	01^{h}30′50.1″	+61°53′37″	6969	6.339(5)	125	7285.517
108 806	HD 10871	–	8.37	01^{h}48′29.1″	+60°26′32″	7634	1.140(2)	45	7209.613
111 164	HD 14795	–	7.64	02^{h}25′26.6″	+60°00′19″	6346	0.6396(7)	32	7323.6586
117 262	HIP 21292	P	8.35	04^{h}34′05.3″	+61°53′03″	5088	0.061237(7)	42	7375.446899

Table B.1. Continued.

ASCC	Identifier	Var. Type[a]	V	RA (J2000)	Dec (J2000)	Nr. Obs.	Period[b] (days)	Amp.[c] (mmag)	Epoch[d] (HJD −2 450 000)
122 680	HIP 33966	–	7.91	07^{h}02′51.3″	+61°18′28″	4073	0.19:	14	7293.6
128 765	HD 101150	P	6.76	11^{h}38′49.1″	+64°20′49″	5067	0.22030(6)	16	7177.50525
129 930	HD 111794	P	7.38	12^{h}50′49.2″	+62°59′10″	6574	0.07968(1)	21	7234.44801
134 035	HIP 80836	P	8.1	16^{h}30′28.3″	+63°34′15″	8512	0.06:	15	7331.385
140 232	HD 186340	P	6.48	19^{h}40′13.2″	+60°30′26″	10689	0.23146(6)	22	7231.67792
141 996	HD 192512	–	7.7	20^{h}11′39.4″	+63°31′39″	10502	5.1(1)	22	7201.6
143 818	TYC 4254-2584-1	–	7.92	20^{h}50′23.0″	+63°50′20″	9603	0.069:	10	7250.512
144 550	HD 201888	–	6.52	21^{h}09′28.8″	+63°17′44″	9574	2.44(1)	15	7172.67
151 816	TYC 4284-529-1	E	8.31	23^{h}28′18.1″	+63°23′27″	8817	1.6295(5)	230	7271.5364
159 418	HIP 3954	P	8.28	00^{h}50′46.4″	+58°44′40″	9404	0.717(2)	19	7257.603
162 612	HD 8026	P	7.93	01^{h}20′47.9″	+56°12′26″	8777	0.561(5)	20	7293.455
166 092	TYC 3688-1817-1	P	8.39	01^{h}53′52.2″	+56°11′11″	7736	0.16:	22	7264.69
174 036	HIP 16448	–	7.97	03^{h}31′53.3″	+56°26′26″	7389	0.41:	16	7265.7
180 189	HIP 27672	–	7.54	05^{h}51′29.2″	+55°15′41″	6557	1.293(7)	25	7375.529
181 723	HD 43812	P	6.08	06^{h}22′03.6″	+59°22′20″	5094	0.19598(3)	20	7060.52291
185 092	HIP 37346	P	7.22	07^{h}39′58.6″	+59°33′48″	4857	0.21282(5)	20	7380.51455
191 012	HIP 57209	–	8.0	11^{h}43′50.9″	+58°24′40″	6287	0.0801(4)	21	7118.6369
199 618	HIP 87405	P	7.04	17^{h}51′44.7″	+56°07′13″	12178	0.058:	9	7192.471
201 832	TYC 3926-224-1	E	7.41	18^{h}43′45.7″	+57°56′53″	11164	0.61747(6)	160	7208.45625
206 277	HD 188665	–	5.14	19^{h}53′17.4″	+57°31′24″	11962	0.727(1)	10	7232.701
206 912	TYC 3940-1007-1	–	7.58	20^{h}01′29.1″	+56°00′23″	11861	0.18:	8	7143.63
209 349	HIP 102027	E	7.33	20^{h}40′32.9″	+55°06′25″	12569	1.633(4)	24	7303.556
209 809	HD 199136	–	7.48	20^{h}52′43.2″	+56°35′06″	11172	0.55:	11	7196.71
214 960	HD 211430	–	7.46	22^{h}15′29.4″	+55°49′07″	12183	2.39(2)	17	7195.53
215 099	HD 211643	–	7.13	22^{h}17′01.0″	+56°10′36″	12092	0.16:	7	7368.37
219 997	TYC 3997-404-1	E	8.1	23^{h}01′27.3″	+58°15′51″	10553	3.385(5)	88	7192.616
221 086	HIP 114516	–	8.27	23^{h}11′41.3″	+56°09′15″	10198	3.7:	18	7331.7
224 040	TYC 4004-1831-1	–	7.97	23^{h}44′42.5″	+55°23′33″	10819	19:	83	7379
229 437	TYC 3261-1837-1	P	7.86	00^{h}38′43.8″	+51°23′28″	13345	0.096:	13	7347.464
235 349	HIP 8877	–	7.98	01^{h}54′19.9″	+52°39′18″	10597	0.038:	10	7293.655
237 369	TYC 3306-2085-1	P	7.72	02^{h}16′08.0″	+51°52′58″	10469	0.5258(9)	21	7301.5375
239 910	HIP 13076	–	7.76	02^{h}48′03.1″	+51°33′06″	11030	0.13:	10	7328.59
245 937	HIP 25316	E	8.27	05^{h}24′55.1″	+50°58′54″	8502	7.189(1)	433	7281.703
258 522	HD 116171	–	8.35	13^{h}20′55.0″	+52°42′42″	12446	0.085:	11	7195.564
259 853	HD 127029	–	7.98	14^{h}27′18.7″	+53°18′39″	14146	3.9:	27	7123.4
271 738	HD 187767	–	7.09	19^{h}49′04.0″	+53°46′03″	15480	1.255(6)	15	7223.575
272 749	HD 190464	P	8.3	20^{h}02′22.9″	+54°40′08″	13543	0.052491(1)	88	7279.536594
273 103	HD 191329	–	6.53	20^{h}07′11.4″	+50°13′47″	17599	0.1892(1)	10	7214.4406
275 394	HIP 101332	–	7.43	20^{h}32′17.0″	+54°09′23″	14689	0.043361(4)	24	7238.445415
276 258	TYC 3955-608-1	P	7.96	20^{h}41′53.6″	+54°25′09″	13978	0.20671(6)	39	7146.64549
278 135	HD 203320	E	6.83	21^{h}19′40.8″	+53°03′29″	15488	0.8553(4)	30	7223.5672

Table B.1. Continued.

ASCC	Identifier	Var. Type[a]	V	RA (J2000)	Dec (J2000)	Nr. Obs.	Period[b] (days)	Amp.[c] (mmag)	Epoch[d] (HJD −2 450 000)
278 375	HD 203819	*	7.86	$21^h22'43.0''$	$+54°13'50''$	14175	2.58(2)	26	7238.73
278 546	HD 204194	–	7.8	$21^h25'23.1''$	$+51°07'58''$	16147	0.1161(3)	17	7324.5286
282 248	HIP 108609	P	7.58	$22^h00'07.2''$	$+51°31'06''$	15838	0.11(7)	16	7163.66
286 887	HD 213495	P	7.92	$22^h30'35.6''$	$+53°31'43''$	14526	0.09748(2)	31	7131.74001
296 032	TYC 3647-1524-1	E	8.23	$23^h55'31.4''$	$+50°19'17''$	14482	6.833(2)	366	7257.512
310 200	HIP 14349	–	8.23	$03^h05'03.2''$	$+49°43'07''$	11649	0.78:	24	7331.54
316 633	HD 32903	P	6.63	$05^h09'04.4''$	$+49°07'19''$	8175	0.09873(2)	14	7369.52315
318 442	HD 38520	–	8.06	$05^h48'43.9''$	$+45°14'14''$	9262	0.064:	18	7323.68
320 596	TYC 3376-264-1	–	8.29	$06^h28'42.5''$	$+46°21'10''$	10382	0.7032(4)	45	7366.3872
329 984	HD 109068	–	7.65	$12^h31'38.4''$	$+45°13'32''$	11924	0.054:	13	7192.483
345 006	TYC 3556-2199-1	–	8.3	$19^h37'30.0''$	$+45°13'35''$	15891	59(4)	81	7345
346 895	HD 188854	E	7.62	$19^h55'12.0''$	$+46°39'56''$	17650	5.653(5)	93	7343.334
353 692	HD 200177	–	7.33	$21^h00'06.6''$	$+48°40'46''$	17583	1.470(5)	19	7262.551
357 011	HIP 106049	–	6.76	$21^h28'48.5''$	$+49°47'42''$	16174	0.07:	7	7354.316
364 197	TYC 3615-740-1	–	8.16	$22^h26'55.2''$	$+49°42'43''$	16068	2.3934(5)	79	7221.6499
370 584	TYC 3638-2472-1	–	8.32	$23^h39'51.1''$	$+45°26'37''$	13792	93(3)	166	7297
371 575	HD 223660	–	8.1	$23^h51'26.9''$	$+47°45'16''$	14782	2.82(2)	34	7253.66
372 907	TYC 2789-35-1	–	8.32	$00^h09'30.5''$	$+43°03'37''$	13602	0.066:	13	7262.451
386 843	HIP 15313	–	7.5	$03^h17'35.0''$	$+42°40'31''$	11019	0.05384(1)	23	7405.5185
387 520	TYC 2869-1296-1	–	8.0	$03^h26'30.1''$	$+42°16'34''$	10863	3.86(2)	43	7079.34
389 555	HIP 18903	–	7.84	$04^h03'06.6''$	$+41°55'55''$	9255	4.39(3)	32	7347.5
396 191	HIP 26961	–	7.44	$05^h43'17.2''$	$+41°07'22''$	9053	15.7(1)	42	7266.6
396 546	TYC 2916-1903-1	P	8.01	$05^h50'13.9''$	$+40°06'13''$	8775	0.088750(7)	34	7268.68499
403 004	HD 66470	P	7.78	$08^h05'25.2''$	$+41°11'24''$	9118	0.17952(2)	29	7399.56333
404 970	TYC 2990-1530-1	–	8.34	$09^h15'50.4''$	$+44°41'53''$	11036	97.5(7)	237	7328.7
413 967	HIP 78226	–	7.4	$15^h58'25.7''$	$+43°12'49''$	15187	1.141(4)	18	7177.572
418 338	HD 162622	–	8.03	$17^h49'58.8''$	$+41°57'19''$	14179	0.64:	18	7272.43
423 447	HD 178090	–	7.21	$19^h05'25.4''$	$+42°10'40''$	13971	17.91(3)	45	7139.64
430 929	TYC 3158-412-1	–	8.34	$20^h05'14.7''$	$+41°33'47''$	13826	34.8(2)	101	7257.6
434 238	HIP 100989	–	7.68	$20^h28'30.7''$	$+43°31'23''$	15349	0.37:	14	7212.66
435 300	HIP 101703	E	8.12	$20^h36'50.9''$	$+44°54'40''$	16323	10.235(5)	276	7325.459
435 960	TYC 3170-536-1	P	8.1	$20^h43'07.7''$	$+40°47'22''$	13757	0.10428(3)	24	7139.73466
437 526	HD 199892	P	6.16	$20^h58'30.9''$	$+41°56'24''$	14054	1.136(1)	31	7199.596
440 889	HIP 106144	P	7.34	$21^h29'59.8''$	$+41°30'38''$	13202	0.1:	11	7207.54
460 027	HIP 8138	P	7.3	$01^h44'38.7''$	$+36°56'18''$	9430	0.041773(2)	29	7386.489021
469 170	HD 25271	P	7.73	$04^h02'29.4''$	$+39°05'50''$	8896	0.060208(6)	25	7398.461248
470 773	HIP 21405	E	8.24	$04^h35'41.0''$	$+39°44'04''$	8219	3.361(1)	124	7369.52
470 842	HIP 21628	–	7.61	$04^h38'38.7''$	$+38°26'55''$	8183	8.59(6)	32	7282.72
475 473	HIP 26249	E	7.6	$05^h35'27.6''$	$+37°54'05''$	8698	0.9656(2)	66	7377.5903
476 068	HD 37737	E	8.06	$05^h42'31.2''$	$+36°12'01''$	9050	7.847(8)	80	7406.44
478 908	TYC 2930-866-1	–	7.74	$06^h15'17.3''$	$+39°56'46''$	9677	51.0(2)	284	7307.6

Table B.1. Continued.

ASCC	Identifier	Var. Type[a]	V	RA (J2000)	Dec (J2000)	Nr. Obs.	Period[b] (days)	Amp.[c] (mmag)	Epoch[d] (HJD −2 450 000)
481 502	HD 48493	–	8.02	06^{h}45′27.7″	+38°22′58″	9903	0.604(2)	24	7389.535
481 932	TYC 2942-1791-1	E	8.34	06^{h}50′50.1″	+37°33′45″	9832	1.17999(5)	362	7347.65609
483 264	HIP 34546	E	6.76	07^{h}09′25.7″	+36°33′48″	9959	0.4043(1)	19	7330.7637
486 406	HIP 39785	–	7.09	08^{h}07′48.5″	+38°34′50″	8979	0.0383566(6)	22	7374.7011397
487 446	HD 71636	E	7.88	08^{h}29′56.3″	+37°04′16″	8806	2.5066(2)	205	7430.3344
487 778	HIP 42341	P	7.46	08^{h}37′56.2″	+39°38′41″	10007	0.1721(2)	16	7394.5066
492 412	HD 97731	E	7.55	11^{h}15′03.1″	+37°34′43″	10510	0.7948(2)	29	7386.696
493 806	HD 106593	P	7.67	12^{h}15′29.1″	+38°39′35″	11582	0.089196(6)	23	7408.606839
501 095	HD 150462	–	7.62	16^{h}39′45.2″	+35°30′56″	11825	4.37(2)	26	7175.69
503 872	TYC 2614-2180-1	–	8.21	17^{h}41′37.9″	+35°21′03″	12217	40.7(9)	133	7393.8
505 542	HD 166276	–	7.72	18^{h}07′59.3″	+39°55′24″	13528	0.05(3)	16	7079.64
505 978	HD 167349	–	7.82	18^{h}13′16.3″	+35°11′49″	12204	0.15:	9	7200.61
510 212	HIP 93311	P	7.8	19^{h}00′22.1″	+37°59′45″	12321	0.23392(6)	36	7225.40442
529 983	HIP 103452	–	7.47	20^{h}57′35.6″	+39°39′46″	11808	1.579(2)	32	7149.589
530 534	TYC 2713-1246-1	P	8.06	21^{h}00′55.4″	+37°21′52″	11434	0.061019(5)	45	7195.606921
530 900	HIP 103915	–	8.09	21^{h}03′17.5″	+38°09′10″	11687	1.626(6)	43	7211.73
545 985	HIP 115621	–	7.68	23^{h}25′20.5″	+36°09′52″	10078	6.16(4)	44	7232.65
550 134	HD 3474	–	8.4	00^{h}37′59.0″	+32°12′48″	10517	0.43:	13	7271.71
554 505	HIP 9039	–	7.9	01^{h}56′26.9″	+30°26′23″	9196	0.702(1)	19	7240.69
555 687	TYC 2314-379-1	–	8.26	02^{h}18′36.4″	+32°07′38″	10205	105.1(3)	319	7343.4
556 920	HD 16511	–	7.66	02^{h}39′50.4″	+33°56′57″	9109	0.2652(2)	17	7407.4604
560 819	HD 25999	E	7.5	04^{h}08′18.2″	+32°27′36″	8895	2.334(4)	31	7389.623
561 947	HD 28271	E	6.37	04^{h}28′52.0″	+30°21′42″	8220	0.46125(6)	26	7330.68858
605 258	HD 173815	P	7.25	18^{h}45′49.8″	+34°31′07″	12107	0.2315(2)	12	7251.3996
609 871	TYC 2653-490-1	–	7.4	19^{h}16′43.5″	+31°08′22″	12184	19.63(1)	90	7462.74
618 172	HIP 97907	–	7.01	19^{h}53′47.3″	+34°35′02″	12055	0.3605(3)	13	7324.4049
619 990	HD 190001	E	7.98	20^{h}01′43.4″	+33°04′01″	11887	0.4044(7)	19	7180.5152
639 599	HIP 109983	–	7.86	22^{h}16′33.6″	+34°31′18″	11133	0.054:	13	7213.636
645 017	HIP 115545	P	8.05	23^{h}24′17.7″	+30°45′05″	10455	0.049867(3)	43	7344.323534
646 882	TYC 2772-1716-1	–	8.2	23^{h}56′58.1″	+32°20′14″	10585	33:	169	7249
650 192	TYC 1746-1184-1	P	8.12	01^{h}03′40.8″	+29°30′03″	9815	0.934(1)	43	7381.336
652 252	HD 11079	–	6.9	01^{h}49′27.2″	+26°28′22″	9221	0.547(1)	13	7407.374
654 547	TYC 1775-633-1	–	8.14	02^{h}38′30.1″	+27°30′55″	8939	21.2(2)	146	7390.5
659 250	HD 27796	–	7.74	04^{h}24′25.5″	+29°01′11″	8276	24.0(2)	126	7366.3
668 059	HD 45784	P	8.09	06^{h}30′45.6″	+29°49′43″	8592	0.082218(7)	27	7370.653738
685 360	HD 110628	P	6.66	12^{h}43′18.5″	+26°07′36″	11712	0.12:	8	7397.69
694 532	TYC 2072-724-1	–	8.14	17^{h}04′47.3″	+28°40′44″	12018	39.8(4)	118	7086.6
699 161	HD 165398	–	7.17	18^{h}04′39.1″	+27°06′55″	12071	0.632(2)	11	7143.528
699 589	HD 166435	–	6.84	18^{h}09′21.3″	+29°57′06″	12788	3.58(3)	22	7273.38
700 708	HD 168874	–	6.99	18^{h}20′49.2″	+27°31′48″	12556	0.87:	11	7286.4
702 739	HD 172244	–	6.91	18^{h}37′59.9″	+28°37′48″	12072	3.88(1)	33	7213.54

Table B.1. Continued.

ASCC	Identifier	Var. Type[a]	V	RA (J2000)	Dec (J2000)	Nr. Obs.	Period[b] (days)	Amp.[c] (mmag)	Epoch[d] (HJD −2 450 000)
716 132	HD 189213	P	7.29	$19^h57'54.5''$	$+28°52'27''$	11764	0.056848(3)	26	7165.566738
719 911	HD 194111	E	8.19	$20^h22'51.4''$	$+27°07'54''$	11011	1.879(4)	27	7277.37
722 510	TYC 2178-1152-1	–	7.99	$20^h40'09.0''$	$+27°04'33''$	11656	5.18(2)	43	7209.54
737 980	HD 221904	–	7.36	$23^h35'55.5''$	$+27°51'54''$	10402	1.268(4)	20	7283.363
745 650	HD 15952	–	8.36	$02^h34'38.7''$	$+24°53'34''$	8603	0.45:	20	7279.63
759 572	TYC 1327-941-1	E	8.15	$06^h23'20.4''$	$+21°59'18''$	8729	6.617(2)	205	7343.671
766 550	HIP 35909	–	7.44	$07^h24'08.8''$	$+21°27'27''$	8822	1.859(2)	27	7389.558
776 651	HD 97005	P	7.48	$11^h10'21.0''$	$+22°42'07''$	9855	0.11728(5)	16	7413.59819
786 454	HIP 81246	–	8.3	$16^h35'39.1''$	$+24°19'38''$	12176	0.089:	10	7118.645
788 621	HIP 84262	P	7.66	$17^h13'30.1''$	$+22°44'45''$	12881	0.08122(1)	20	7230.47551
792 736	HD 164900	–	6.21	$18^h02'30.2''$	$+22°55'24''$	12050	1.5(5)	11	7198.7
792 889	TYC 2091-3605-1	P	8.26	$18^h04'13.8''$	$+23°26'48''$	12121	0.07947(2)	21	7154.69444
795 006	HD 169490	–	6.74	$18^h24'05.6''$	$+20°27'08''$	11421	0.042:	7	7213.475
795 152	HD 169798	–	6.78	$18^h25'27.9''$	$+22°42'25''$	11446	1.567(5)	17	7240.504
802 089	HIP 95131	–	7.41	$19^h21'17.3''$	$+20°57'46''$	11277	1.7:	12	7264.5
803 943	HIP 96767	–	7.52	$19^h40'11.7''$	$+23°53'06''$	11401	0.379(1)	14	7195.579
804 978	TYC 2139-874-1	E	8.17	$19^h47'53.7''$	$+24°14'04''$	11110	3.364(1)	118	7220.508
805 448	HD 187730	P	6.72	$19^h50'45.1''$	$+20°12'41''$	11372	0.070557(6)	19	7304.490169
809 501	HIP 99767	E	7.47	$20^h14'30.5''$	$+24°50'41''$	11147	6.39(1)	41	7255.5
810 232	HD 193325	–	7.51	$20^h19'01.0''$	$+20°27'51''$	10948	3.15(1)	26	7165.61
815 261	HIP 102836	–	7.95	$20^h50'01.1''$	$+20°52'48''$	10910	2.53(2)	26	7291.44
815 767	TYC 2175-204-1	P	8.37	$20^h53'42.4''$	$+24°37'03''$	10493	0.11893(2)	34	7214.6974
833 678	HIP 9924	E	6.61	$02^h07'46.0''$	$+18°01'46''$	8356	2.575(1)	47	7343.487
834 693	HIP 12441	–	7.97	$02^h40'09.0''$	$+16°43'37''$	8102	1.157(6)	23	7384.407
838 077	HIP 19763	–	8.14	$04^h14'15.0''$	$+18°53'39''$	8531	0.36:	17	7295.59
845 608	HD 42476	E	7.51	$06^h11'39.0''$	$+17°22'39''$	8775	2.6276(8)	64	7271.6655
856 484	HIP 37685	–	7.27	$07^h43'53.5''$	$+15°15'28''$	7763	0.16:	11	7385.6
871 363	HIP 72976	P	7.13	$14^h54'50.0''$	$+15°19'31''$	10311	1.673(2)	22	7151.645
872 286	HIP 75340	P	7.92	$15^h23'41.5''$	$+17°52'01''$	11173	0.11:	12	7213.46
881 859	HIP 89196	P	8.09	$18^h12'10.9''$	$+19°05'37''$	11462	0.16:	12	7431.73
886 302	HD 175428	–	7.08	$18^h54'48.3''$	$+15°20'34''$	10879	0.4085(6)	12	7293.3683
889 987	HD 184502	–	7.02	$19^h34'18.7''$	$+16°15'54''$	10533	4.297(9)	35	7168.6
893 583	HD 188328	E	7.16	$19^h54'02.0''$	$+15°17'32''$	11188	0.13650(2)	20	7249.62863
899 268	HD 195775	–	6.96	$20^h32'43.7''$	$+16°46'02''$	11186	2.240(8)	27	7220.608
911 414	HIP 115847	P	7.41	$23^h28'12.8''$	$+18°32'18''$	8833	0.17253(7)	18	7196.58419
914 998	HD 5843	P	8.05	$01^h00'13.2''$	$+11°56'07''$	9105	0.07903(1)	41	7265.52566
916 845	HD 11432	–	7.98	$01^h52'37.1''$	$+12°26'34''$	8119	0.18:	14	7324.38
922 992	HIP 23629	–	7.61	$05^h04'49.1''$	$+13°18'32''$	8257	1.648(3)	26	7085.382
924 214	HD 35909	P	6.34	$05^h28'34.8''$	$+13°40'44''$	8271	0.0394490(9)	21	7424.3453195
940 994	HIP 36843	–	7.74	$07^h34'32.0''$	$+12°18'17''$	8061	1.784(2)	24	7381.756
960 255	HD 142553	–	7.69	$15^h54'49.0''$	$+11°30'55''$	12593	0.7966(6)	28	7096.7156

Table B.1. Continued.

ASCC	Identifier	Var. Type[a]	V	RA (J2000)	Dec (J2000)	Nr. Obs.	Period[b] (days)	Amp.[c] (mmag)	Epoch[d] (HJD −2 450 000)
960 597	HIP 78713	–	8.0	16^{h}04′08.3″	+10°00′23″	13590	83(1)	107	7183
960 637	HIP 78779	–	8.3	16^{h}04′58.8″	+10°56′54″	13261	0.1:	19	7231.54
960 825	TYC 949-516-1	P	8.19	16^{h}09′43.4″	+10°26′44″	13545	0.11696(2)	28	7130.59871
972 871	HIP 92236	–	7.51	18^{h}47′53.5″	+11°09′49″	12215	1.091(2)	24	7144.643
975 722	HIP 94430	–	8.34	19^{h}13′09.5″	+12°01′22″	12192	2.95(1)	44	7196.42
992 878	HD 205355	P	8.1	21^{h}34′26.2″	+10°26′05″	11510	0.09856(4)	22	7196.52782
995 573	HD 211856	E	7.61	22^{h}19′55.4″	+12°27′07″	9563	2.252(7)	34	7237.606
1 000 278	HD 231	–	7.44	00^{h}07′04.2″	+06°52′32″	10936	0.52:	12	7325.48
1 009 402	HIP 21304	–	8.31	04^{h}34′22.4″	+08°11′14″	9240	0.049:	13	7428.418
1 011 428	HIP 23666	–	7.44	05^{h}05′13.0″	+08°56′32″	10797	0.552(1)	17	7067.443
1 015 212	HD 40188	P	7.84	05^{h}57′27.7″	+05°00′04″	9898	0.14747(2)	35	7121.36972
1 021 140	HD 47416	–	7.76	06^{h}38′51.1″	+07°58′18″	10286	3.56(2)	32	7287.75
1 028 333	TYC 763-226-1	P	8.33	07^{h}21′32.9″	+08°54′54″	10790	0.11708(9)	31	7379.54026
1 031 582	HIP 38043	–	7.51	07^{h}47′50.1″	+07°20′29″	10701	3.84(1)	29	7332.69
1 034 441	HD 71310	P	7.12	08^{h}27′00.0″	+07°13′16″	11609	0.08655(3)	17	7374.51963
1 036 076	HD 75811	–	6.34	08^{h}52′24.1″	+05°20′26″	12384	0.943(4)	13	7418.394
1 040 348	HD 92151	–	7.37	10^{h}38′27.6″	+05°54′49″	10958	0.074(1)	15	7435.643
1 046 116	TYC 900-482-1	P	8.13	13^{h}51′29.9″	+08°20′39″	14110	0.04424(9)	25	7150.54116
1 051 776	HD 145589	P	6.51	16^{h}11′29.7″	+09°42′43″	13639	0.13:	7	7263.44
1 069 398	HD 178165	E	7.21	19^{h}07′20.7″	+05°13′08″	13762	1.3932(6)	54	7268.461
1 074 782	HIP 97510	–	7.68	19^{h}49′9.5″	+08°16′38″	14236	0.064:	14	7251.468
1 080 495	HD 195634	P	7.98	20^{h}32′24.1″	+05°16′28″	11649	0.18412(5)	41	7216.67118
1 081 225	TYC 1088-122-1	–	8.18	20^{h}38′36.8″	+08°57′03″	13753	0.64:	20	7260.52
1 096 601	HD 10165	–	7.65	01^{h}39′25.1″	+00°36′44″	6150	1.4:	22	7265.6
1 099 196	HD 17779	P	7.38	02^{h}51′20.8″	+03°03′25″	7041	0.093(7)	16	7274.744
1 101 515	HD 24181	–	7.67	03^{h}51′03.8″	+01°43′30″	6940	0.3994(1)	41	7240.7324
1 103 850	HD 30234	P	7.97	04^{h}45′56.3″	+04°21′36″	9084	0.14:	19	7304.55
1 105 156	HD 32359	–	7.31	05^{h}02′44.6″	+03°27′28″	8238	0.786(2)	21	7097.384
1 106 000	HD 33883	–	6.12	05^{h}13′31.5″	+01°58′03″	7393	0.2232(2)	10	7302.6442
1 110 887	HD 43021	–	7.82	06^{h}14′10.4″	+02°34′29″	6874	0.08240(3)	25	7418.53627
1 112 596	HD 45853	–	8.1	06^{h}30′04.4″	+01°19′41″	7163	0.14:	14	7325.56
1 124 002	HD 60155	–	7.4	07^{h}33′13.7″	+00°09′52″	6713	3.7:	20	7331.7
1 135 311	HD 90775	P	7.43	10^{h}28′58.7″	+02°38′48″	7834	0.06184(1)	22	7152.47346
1 141 467	HD 118578	P	6.65	13^{h}37′44.0″	+02°22′56″	8671	0.27937(2)	39	7184.50913
1 146 792	HD 141610	–	7.15	15^{h}49′51.6″	+02°30′03″	9579	0.037684(5)	14	7126.587781
1 153 518	HD 158352	–	5.41	17^{h}28′49.7″	+00°19′50″	8335	0.07561(1)	10	7142.70966
1 155 325	HD 162178	E	7.53	17^{h}49′35.8″	+04°22′36″	14160	2.609(1)	78	7220.449
1 171 650	HD 195533	P	7.2	20^{h}31′43.6″	+04°24′57″	11662	0.0696(3)	18	7164.6843
1 178 919	HD 208818	–	8.13	21^{h}58′57.6″	+00°05′44″	7950	0.073:	16	7286.491
1 201 273	HD 43157	–	5.82	06^{h}14′36.7″	−04°34′06″	6108	2.609(3)	28	7428.486
1 203 415	HD 46487	–	5.09	06^{h}33′37.9″	−01°13′12″	7051	0.26670(6)	15	7350.63681

Table B.1. Continued.

ASCC	Identifier	Var. Type[a]	V	RA (J2000)	Dec (J2000)	Nr. Obs.	Period[b] (days)	Amp.[c] (mmag)	Epoch[d] (HJD −2 450 000)
1 223 786	HD 77266	P	7.81	09^{h}01′23.1″	−03°22′05″	6492	0.12:	21	7406.44
1 236 357	HD 134250	P	8.24	15^{h}08′57.7″	−04°00′48″	7604	0.044554(2)	43	7068.628
1 245 743	HD 177705	E	8.37	19^{h}05′54.7″	−00°41′06″	9267	8.693(3)	246	7256.362
1 248 591	HD 185004	P	8.38	19^{h}37′12.0″	−03°28′29″	6914	0.08:	33	7303.378
1 255 981	HD 201222	–	6.87	21^{h}08′09.4″	−00°59′23″	7981	0.05747(1)	14	7175.66204
1 257 572	HD 205244	P	6.68	21^{h}34′07.6″	−04°22′05″	7082	0.039267(4)	16	7324.347321
1 269 152	HD 17056	–	7.92	02^{h}44′09.1″	−06°24′50″	4532	47:	212	7337
1 276 505	HD 35281	–	6.11	05^{h}23′18.5″	−08°24′56″	4778	0.542(1)	17	7331.637
1 280 725	HD 44721	–	7.79	06^{h}23′00.4″	−06°31′58″	4971	52.0(7)	147	7098.4
1 322 909	HD 168856	E	7.05	18^{h}22′10.8″	−07°29′55″	5921	2.427(5)	36	7227.49
1 332 964	HD 190795	P	7.77	20^{h}07′03.6″	−08°10′54″	4869	0.10378(3)	28	7220.66463
1 398 472	HD 131716	–	8.02	14^{h}55′31.1″	-10°16′53″	4888	0.045:	19	7141.662
1 418 643	HD 194285	–	7.41	20^{h}25′08.1″	-11°42′17″	4305	0.13(8)	20	7161.62
1 420 399	HD 198258	P	7.73	20^{h}49′25.1″	-11°27′18″	4478	0.12:	19	7256.58
1 443 715	HD 42097	–	8.18	06^{h}08′05.8″	-19°46′24″	2925	0.13733(2)	53	7414.4725
1 448 655	HD 50463	–	7.13	06^{h}52′46.0″	-16°12′44″	2434	3.52(1)	38	7094.35
1 476 664	HD 97635	–	7.79	11^{h}14′03.7″	-15°26′07″	3602	0.082:	20	7138.521
1 484 762	HD 129978	–	6.34	14^{h}45′57.8″	-15°27′34″	2991	0.24:	12	7143.66
1 510 357	HD 190756	–	7.85	20^{h}07′03.7″	-17°11′42″	2991	1.4:	29	7203.6
1 524 727	HD 15807	P	7.91	02^{h}32′00.1″	-23°05′04″	2354	0.1097(4)	34	7386.3143
1 534 408	HD 39366	–	7.84	05^{h}51′10.4″	-23°25′10″	2498	0.0394(2)	27	7408.437
1 550 166	HD 60054	E	7.88	07^{h}31′51.1″	-20°55′49″	3449	8.073(4)	237	7057.421
1 554 048	HD 63127	–	7.48	07^{h}46′26.9″	-21°32′44″	3022	46.7(3)	199	7123.4
1 564 203	HD 74298	P	7.81	08^{h}42′33.6″	-22°23′10″	2948	0.1923(2)	29	7433.5139
1 571 309	HD 89638	E	7.47	10^{h}20′13.2″	-23°06′09″	3133	0.66700(7)	87	7407.66507
1 574 120	HD 98252	–	8.09	11^{h}17′55.2″	-22°25′53″	3129	0.12:	23	7134.5
1 607 170	HD 191579	–	8.34	20^{h}11′28.7″	-24°13′37″	2576	0.073:	26	7330.321
1 612 842	HD 209475	–	7.85	22^{h}04′9.9″	-21°46′48″	2415	0.048:	22	7258.517
1 623 560	HD 23616	P	6.97	03^{h}45′33.1″	-25°54′56″	2588	0.056071(3)	34	7428.400956
1 669 230	HD 97111	–	7.31	11^{h}10′31.8″	-25°59′45″	3136	0.06566(2)	22	7134.37362
1 670 986	HD 102593	P	7.93	11^{h}48′30.5″	-25°05′09″	3452	0.0609(6)	31	7160.4754
1 682 378	HD 141831	P	7.22	15^{h}52′04.5″	-26°31′23″	3939	0.07958(2)	32	7086.68994
1 684 892	HD 149980	P	7.14	16^{h}39′16.4″	-29°55′27″	3185	0.12037(2)	31	7151.679
1 688 280	HD 156780	–	7.08	17^{h}20′30.7″	-26°32′59″	3697	86:	72	7145
1 769 029	HD 118972	–	6.92	13^{h}41′04.0″	-34°27′50″	2589	9.56(8)	54	7136.46
1 778 918	HD 147148	–	8.27	16^{h}21′15.9″	-30°06′04″	3353	0.048:	27	7178.569
1 793 476	HD 169660	–	7.28	18^{h}27′03.8″	-31°22′21″	3430	38(1)	108	7308